MASTER THESIS

ENERGY TECHNOLOGY FOR SUSTAINABLE DEVELOPENT

Thermodynamic Analysis of a High Temperature Heat Pump coupled with an Organic Rankine Cycle for Energy Storage

AUTHOR: **LINDEMAN, LUKAS**

SUPERVISOR: HASSAN, ABDELRAHMAN HUSSEIN

UPV TUTOR: CORBERÁN SALVADOR, JOSÉ MIGUEL

Academic Year: 2017-18

"July 2018"

ACKNOWLEDGEMENTS

First, I would like to thank Prof. José Miguel Corberán Salvador for helping me during this year and for giving me the opportunity to be part of this project.

Secondly, I would like to thank Dr. Abdelrahman Hussein Hassan for giving me tremendous support and valuable guidance during this work. I am very thankful for the feedback he has given me and the discussions we have had during this project.

Finally, I would like to thank my mother and father for the love and support they have always given me. Without them this would not have been possible.

The current thesis has been implemented within the framework of the CHESTER project, which has received funding from the European Union's Horizon 2020 research and innovation program under grant agreement No 764042

RESUMEN

La transición energética hacia las energías renovables requiere de nuevas soluciones para el almacenamiento de energía, ya que las tecnologías de almacenamiento existentes están asociadas con desventajas como el tiempo de descarga, el coste, el uso del terreno etc. Este trabajo está enmarcado dentro del proyecto Europeo CHESTER (**C**ompressed **H**eat **E**nergy **ST**orage for **E**nergy from **R**enewable sources). Cuando hay exceso de energía eléctrica en la red, el sistema de almacenamiento térmico utiliza una bomba de calor (HP) para aumentar la temperatura del calor residual y almacenarlo. El sistema de almacenamiento es un sistema latente (LHS) mediante materiales de cambio de fase (PCM) y un sistema de almacenamiento sensible (SHS) mediante dos tanques de agua. Cuando la red demanda energía eléctrica, el sistema de almacenamiento a alta temperatura se utiliza acoplado a un ciclo orgánico de Rankine (ORC) para producir electricidad.

Para evaluar la eficiencia del sistema se ha desarrollado un modelo termodinámico, con el que se han analizado: tres temperaturas de cambio de fase del PCM (133, 149 y 183 °C), la configuración de la bomba de calor y del sistema ORC y varias características de los fluidos refrigerantes, especialmente la pendiente de la curva de vapor saturado del refrigerante.

Los resultados indican que los fluidos isoentrópicos tienen el mejor comportamietno, siendo el R1233zd(E) considerado como el mejor fluido de trabajo para bajas y medias temperaturas de fusión. Para una temperatura de fusión de 133 °C y una temperatura de la fuente de calor de 75 °C, una eficiencia igual a 1 del ciclo completo puede ser alcanzada. Para alta temperatura el fluido con mejor comportamiento es el R141b. Fluidos secos como el HFO1336mzz(Z) y el ciclopentano presentan el peor comportamiento de los fluidos seleccionados. No se considera beneficioso para el sistema un ciclo con dos etapas de compresión ni tampoco un ciclo ORC con procesos de recuperación o regeneración.

Palabras calves: Almacenamiento térmico, bombas de calor de alta temperatura, ciclo orgánico de Rankine, modelado numérico.

RESUM

La transició energètica cap a les energies renovables requerix de noves solucions per a l'emmagatzemament d'energia, ja que les tecnologies d'emmagatzemament existents estan associades amb desavantatges com el temps de descàrrega, el cost, l'ús del terreny etc. Este treball està emmarcat dins del projecte Europeu CHESTER (Compressed Heat Energy STorage for Energy from Renewable sources). Quan hi ha excés d'energia elèctrica en la xarxa, el sistema d'emmagatzemament tèrmic utilitza una bomba de calor (HP) per a augmentar la temperatura de la calor residual i emmagatzemar'l-ho. El sistema d'emmagatzemament és un sistema latent (LHS) per mitjà de materials de canvi de fase (PCM) i un sistema d'emmagatzemament sensible (SHS) per mitjà de dos tancs d'aigua. Quan la xarxa demanda energia elèctrica, el sistema d'emmagatzemament a alta temperatura s'utilitza acoplat a un cicle orgànic de Rankine (ORC) per a produir electricitat.

Per a avaluar l'eficiència del sistema s'ha desenvolupat un model termodinàmic, amb el que s'han analitzat: tres temperatures de canvi de fase del PCM (133, 149 i 183 °C) , la configuració de la bomba de calor i del sistema ORC i diverses característiques dels fluids refrigerants, especialment el pendent de la corba de vapor saturat del refrigerant. Els resultats indiquen que els fluids isoentròpics tenen el millor comportament, sent el R1233zd (E) considerat com el millor fluid de treball per a baixes i mitges temperatures de fusió. Per a una temperatura de fusió de 133 °C i una temperatura de la font de calor de 75 °C, una eficiència igual a 1 del cicle complet pot ser aconseguida. Per a alta temperatura el fluid amb millor comportament és el R141b. Fluids secs com el HFO1336mzz (Z) i el ciclopentano presenten el pitjor comportament dels fluids seleccionats. No es considera beneficial per al sistema un cicle amb dos etapes de compressió ni tampoc un cicle

Paraules Claus: Emmagatzemament tèrmic, bombas de calor d'alta temperature, cicle orgànic de Rankine, modelatge numèric.

ABSTRACT

The transition towards an increasing share of renewable energy in the electricity production requires new solutions of energy storage. Existing energy storage technologies can provide good solutions but are also associated with various constraints such as land use, discharge time, cost etc. This thesis has been carried out under the frame of the European project CHESTER (**C**ompressed **H**eat **E**nergy **ST**orage for **E**nergy from **R**enewable sources). During times of excess electricity production, a heat energy storage system uses a heat pump (HP) to pump low-grade thermal energy to a higher temperature reservoir where the heat is stored. The reservoir consists of a latent heat storage (LHS) unit with a phase changing material (PCM) and a Sensible heat storage (SHS) unit with two water tanks. At times of insufficient electricity production, the stored energy is used to operate an organic Rankine cycle (ORC) to produce electricity.

A thermodynamic model has been developed to evaluate the system performance. Three different melting temperatures of the PCM (133, 149 and 183 °C) are evaluated as well as some characteristics of the working fluid, especially the slope of the saturated vapor curve (dry, isentropic or wet fluid). The system configuration of the HP and the ORC are also analyzed.

The results indicated that isentropic fluids have the best overall system performance. R1233zd(E) is considered to be the best working fluid for the low and medium melting temperatures. For a melting temperature of 133 °C, a roundtrip efficiency of 1 can be reached if the source temperature is 75 °C. For the high temperature storage, R141b is the best working fluid. Dry fluids such as HFO1336mzz(Z) and Cyclopentane have the lowest performance of the selected working fluids. A two-stage compression in the HP is not considered to be beneficial for the system, neither is an ORC cycle with recuperation or regeneration processes.

Key words: Thermal storage system, High temperature heat pump, Organic Rankine cycle, Numerical modeling.

TABEL OF CONTENTS

LIST OF FIGURES

LIST OF TABLES

1. INTRODUCTION

1.1 BACKGROUND

Carbon is the source of most of the electricity generation in the world today. CO_2 is released to the atmosphere whenever a carbon-based fuel is combusted and this contributes to the global warming. To reduce the CO_2 emissions, conventional carbon-based electricity generation needs to be phased out to make room for electricity generation from renewable energy sources (RES).

One problem associated with this transition is the intermittency of RES. Since carbon-based fuels such as natural gas or coal have a good storage potential, the electricity generation can be scheduled with a high level of certainty. This is not the case for many RES and therefore it is more difficult to generate electricity to match the demand curve. The future grid will need to adapt to the availability of RES if the electricity generation is going to always meet the demand.

One way of reducing the uncertainty of electricity generation associated with RES is to integrate energy storage solutions in the grid. Whenever the supply of electricity is higher than the demand, the excess electricity can be used to charge various energy storage systems that later can be used for electricity generation when the demand is higher than the supply.

Fig. 1 shows some energy storage techniques that can, or has the potential to, be used for energy storage. The area in which the technology is applicable is based on the discharge time and the system power rating. To reduce the large scale and long-term uncertainty from RES, both long discharge time and high system power rating are desirable characteristics.

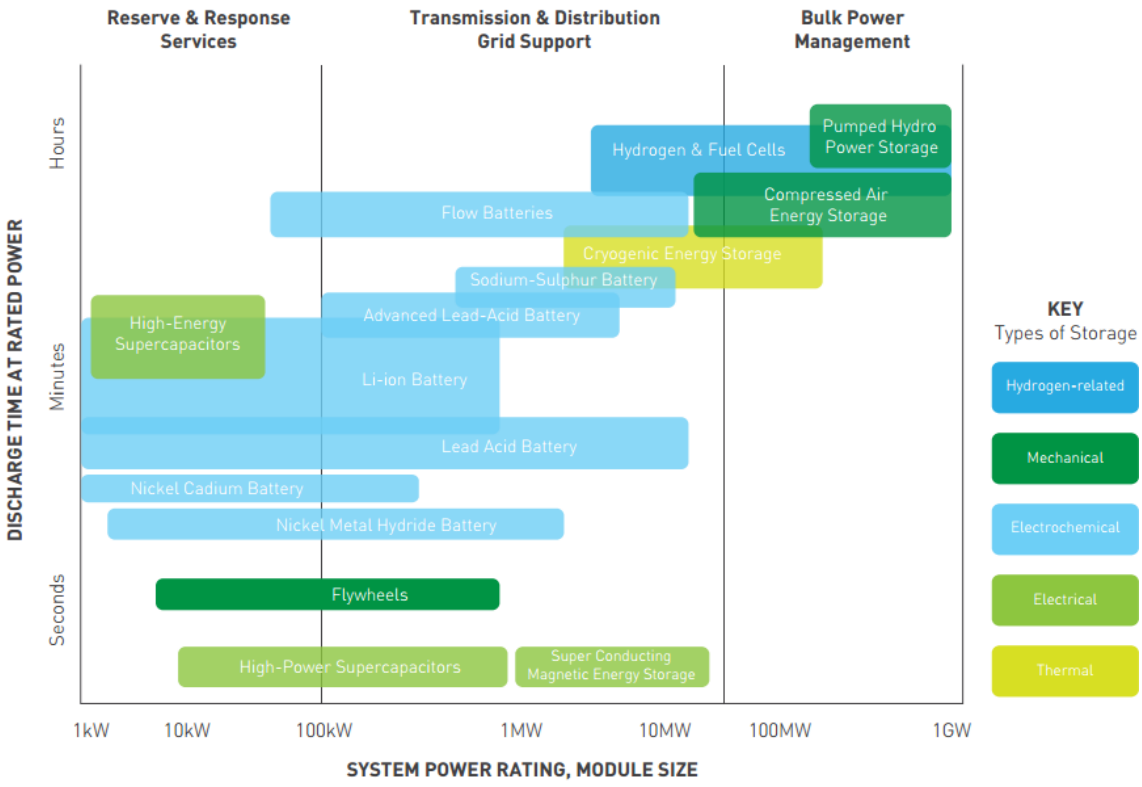

Figure 1. Energy storage technologies based on the discharge time and the system power rating [1].

There are many techniques for energy storage with different levels of maturity explained in literature. Among the techniques suggested in the Fig. 1, Pumped Hydro Storage (PHS) is by far the most mature and widely used technique. When electricity is available at a low price, water is pumped from a lower reservoir to a high reservoir to increase its potential energy. Later, during times with a high price of electricity, the water is released through the turbines to generate electricity. The efficiency of PHS is usually in the range of 65-85 %. PHS is however limited by geological constraints and it needs an appropriate elevation and a good supply of water. [2]

Among the less developed and used systems are Compressed Air Energy Storage (CAES) and Hydrogen Storage. CAES uses excess electricity to compress air into underground caverns or tanks. When electricity is needed, gas is combusted together with the stored high-pressure air and expanded through a turbine to generate electricity. The efficiency of CAES systems are around 70%. Hydrogen Storage uses excess electricity to electrolyze water to create hydrogen. The overall efficiency is low, around 30% and is not yet a mature technology. [2]

1.2 AIMS AND OBJECTIVES

This thesis has been carried out under the frame of the European project CHESTER (**C**ompressed **H**eat **E**nergy **ST**orage for **E**nergy from **R**enewable sources). The CHESTER project pursues the development and evaluation of an innovative, efficient and smart energy storage and management system to provide increased flexibility to the power grid. In addition, it will incorporate advanced features that allow the integration of thermal RES such as solar, biomass, waste heat, geothermal, etc. This system consists of a high-temperature heat pump (HT-HP), a thermal energy storage system (TES), and a heat engine based on organic Rankine cycle (ORC).

Fig. 2 demonstrates a basic schematic of a CHEST system. At time when there is a possibility to produce excess electricity, the low-grade thermal energy, is pumped to a higher heat temperature reservoir, which in this case is the high-temperature thermal storage system with a phase changing material (PCM). This process is called charging process. Later, for high demand periods, the thermal heat stored is used to operate an ORC to produce electricity. This process is called discharging process.

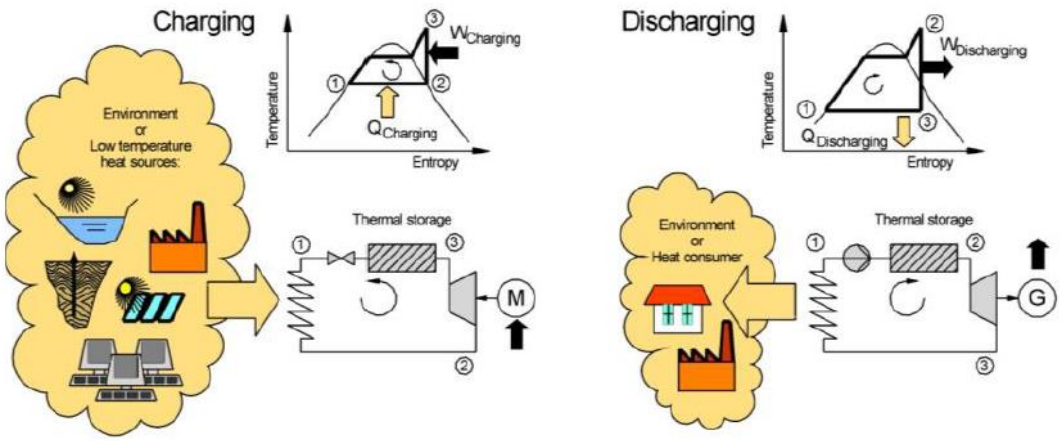

Figure 2. Basic schematic of CHEST [3].

The Integration of RES allows a higher flexibility of the CHEST system, making it capable of efficiently responding under different boundary conditions and needs. Based on the state of boundary conditions the roundtrip efficiency of the system could, in theory, equal or even exceed 100%.

To efficiently charge the high-temperature heat storage system, a HP that operates between evaporation temperature of 30-100 °C and condensation temperature up to 200 °C should be utilized. Later, the fluid of the ORC system evaporates at a temperature below the melting temperature of the PCM. The sink temperature should be as low as possible in order to increase the ORC efficiency hence the overall performance of CHEST system.

The main objective of the current work is to assess the thermodynamic performance of the CHEST system. To achieve this main objective the following specific objectives should be fulfilled:

- Refrigerants comparison and selection
- HT-HP cycle, modelling, and analysis
- ORC cycle, modelling, and analysis
- Numerical model development of the CHEST.
- Validation and parametric studies.

1.3 STATE OF THE ART

A state of the art has been made in order to investigate has been previously done in the field. Focus has been put on the complete charging/discharging system as well as possible configurations of the HP and ORC that would yield a better overall efficiency.

1.3.1 Heat Pump

The basic HP consists of a condenser, an evaporator, a compressor and an expansion valve. However, using a basic HP configuration for applications with a high temperature lift can be problematic. Fig. 3a shows the effect of an increasing condensation temperature in the temperature-entropy (T-s) diagram. It can be seen that the discharge temperature increases if condensation temperature is increased. This can be a problem for lubricating oils used in the compressor, which can dissolve at high temperatures and thereby damage the compressor [4]. Moreover, for piston compressors, the largest possible pressure ratio is around 10 [5], which might be exceeded if large temperature lifts are used.

Fig. 3b shows the effect of increasing the condensation temperature in pressure-enthalpy (P-h) diagram. The figure shows that if the refrigerant is throttled from higher pressures, point (4') move towards the saturated vapor line. This means that the enthalpy at (4') will increase and lead to a smaller evaporation capacity. Fig. 3b also shows that a larger compressor work required to compress the refrigerant to the condensing pressure. Therefore, more advanced cycle configurations are oftentimes used for applications with a high temperature lift.

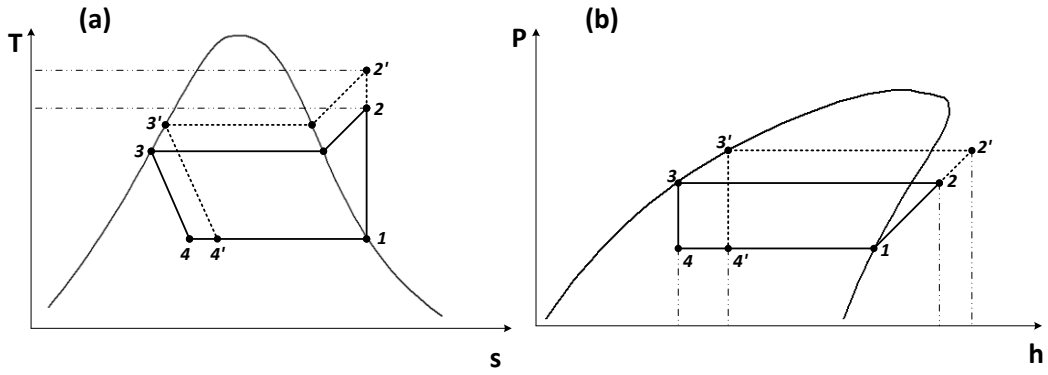

Figure 3. Cycle effects when increasing condensation temperature [6].

One way to reduce the reduce the disadvantages of a large temperature lift is to introduce one or many flash tanks in the system. In Fig. 4a, a flash tank at an intermediate pressure level *(7)* separates the liquid from the vapor during the throttling process. Since the second throttling takes place in saturated conditions *(8)*, the vapor quality at the inlet of the evaporator will be lower hence increasing the refrigeration capacity.

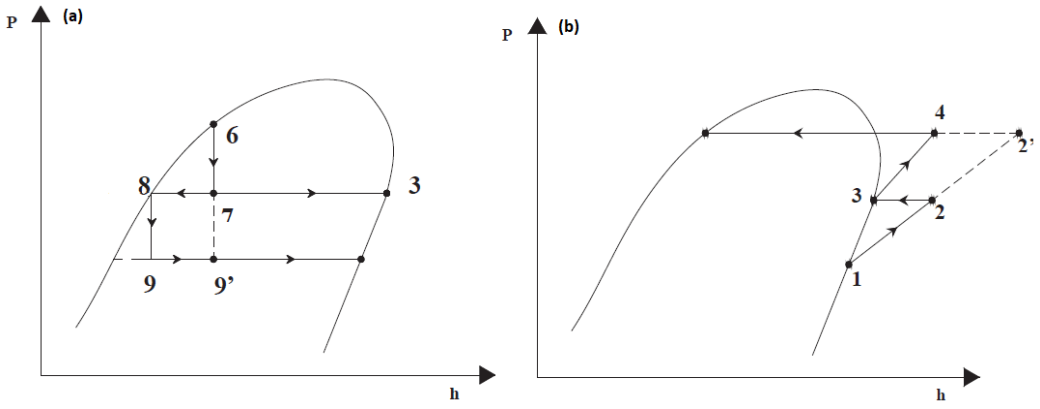

Figure 4. Two stage HP with a flash tank [6].

Fig. 4b shows the effect of a two-stage compression. By interrupting the compression at (2) and cooling the superheated vapor to saturated conditions, the work done by the compressor is reduced. Apart from saving work, the discharge temperature at *(4)* will be lower than in the compression would have continued without interruption *(2')*.

In a combination of these systems, the two-phase liquid-vapor in the flash tank works as a cooler for the superheated vapor at point *(2)*. In Fig. 5a, the superheated vapor at the outlet of the compressor is fed to the flash tank. The vapor and liquid are separated and the second stage compression takes place at saturated vapor conditions. This system is called Flash Gas Intercooler (FGI). In Fig. 5b, the saturated vapor from the flash tank mixes with the superheated vapor after the first expansion. The resulting mixture at *(3)* is a slightly superheated vapor, which is then compressed to the high-pressure level. This system is called Flash Gas Removal (FGR).

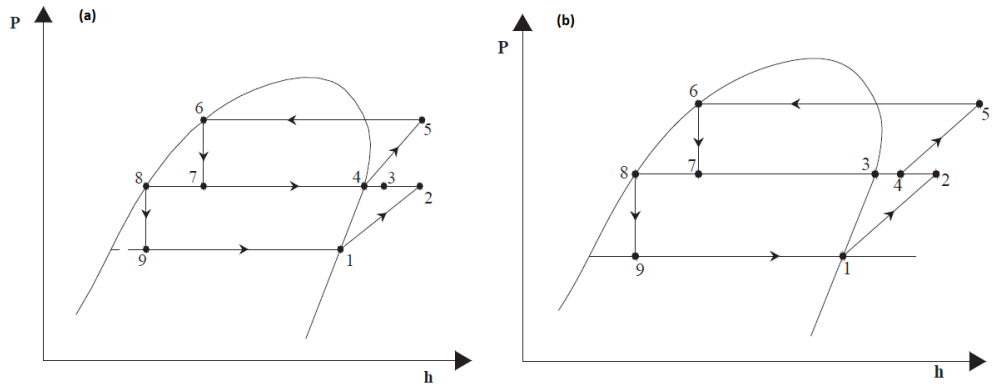

Figure 5. Two stage HP with a flash tank for FGI and FGR [6].

1.3.1.1 High temperature heat pumps

By having explained the basics of multi-compression system, which is common in large temperature lift applications, the following section describes the latest developments in high temperature heat pumps HTHP.

This section is mostly based on the work of Arpagaus et al. [7] which recently wrote an extensive review article about HTHP. According to the them, there is no strict definition of what can be considered as a HTHP. The most common definition in literature is that a heat pump can be considered high temperature is if the condensing temperature is above 100 °C. Heat pumps with a condensation temperature of up to 100 °C are today used in many areas in industry such as processing of paper, food and beverages, chemicals and metal. However, there are many processes in industry that require higher temperatures and there is potential to develop heat pumps to reach higher temperatures. Although HTHP can have good energy efficiency compared to conventional solutions, Arpagaus et al. also pointed out several barriers for a larger commercial implementation. Among these barriers were long payback periods and lack of available refrigerants. Moreover, oftentimes tailor-made designs are required which increase the cost. The lubricating oil used in the piston and screw compressors need to be carefully chosen to prevent boiling, have an appropriate viscosity and be thermic stable at high temperatures.

The benchmark of the commercially available HTHP with the operating refrigerant are shown in Fig. 6.

Manufacturer	Product	Refrigerant	Max. heat sink temperature
Kobe Steel (Kobelco steam grow heat pump)	SGH 165 SGH 120 HEM-HR90,-90A	R134a/R245fa R245fa R134a/R245fa	165 °C 120 °C 90 °C
Vicking Heating Engines AS	HeatBooster S4	R1336mzz(Z) R245fa	150 °C
Ochsner	IWWDSS R2R3b IWWDS ER3b IWWHS ER3b	R134a/ÖKO1 ÖKO (R245fa) ÖKO (R245fa)	130 °C 130 °C 95 °C
Hybrid Energy	Hybrid Heat Pump	R717/R718 (NH_3/H_2O)	120 °C

Figure 6. Commercially available heat pumps with highest heat sink temperature [7].

One of the commercially available heat pumps from the list above that can reach the highest temperatures is the Heat Booster from Viking Heat Engines. It uses the Refrigerant called R1336mzz(Z) with a piston compressor and a polyolester oil for lubrication. According to the website of Viking Heat Engines, The Heat Booster is able reach temperatures of up to 160 °C [8].

Fig. 7 shows some of the ongoing research projects using heat pump a very high sink temperature. Three different cycle types can be seen. Two of the projects use single stage cycle and one of which is adding an internal heat exchanger. Both of these projects are using R1336mzz(Z) as a fluid. The third project uses a flash tank with an injection in the suction chamber to lower the superheating degree. In, this project R718 (Water) is used as the working fluid. The reason for this was its low environmental impact, easily available and it has a high critical temperature [9].

Organisation, Project partners	Cycle type	Refrigerant	Heat source (grey) and heat sink (black) temperatures [°C]
			20 40 60 80 100 120 140 160
Austrian Institute of Technolog Vienna, Chemours, Bitzer	Single-stage with IHX	R1336mzz(Z)	
Austrian Institute of Technolog Vienna, Chemours, Bitzer	Single-stage	R1336mzz(Z)	
PACO, University Lyon, EDF Electricité de France	Flash tank	R718	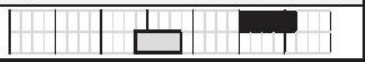

Figure 7. Ongoing projects developing HTHP [7].

1.3.2 Organic Rankine Cycle

Since the proposed storage temperature for the system is 200 °C, an ORC is proposed. An ORC uses a different fluid than water to run what in other ways works much like the conventional water-steam Rankine cycle. For low temperature applications ORCs are preferred since low heat quality restricts evaporation pressure and superheating temperature of the steam-water cycle which leads to lower cycle efficiency, moreover the steam turbine will have a low isentropic efficiency (60-65%) [10]. Among the most common areas where ORCs are used are geothermal, biomass, waste heat applications. The temperature range in which the ORC operates is usually 80-300 °C. For temperatures higher than 300 °C, conventional water-steam Rankine cycles are usually considered a better option [11]. Depending on the application, ORCs can work with a number of different fluids. Some of commonly used fluids are Toluene, Cyclopentane, Ammonia, Butane and Refrigerant R245fa [10].

1.3.2.1 *The Basic ORC*

The basic ORC is the simplest cycle configuration. Fig. 8 shows the schematic of the basic ORC system with the corresponding T-s diagram. Heat from a temperature source *(7) -> (8)* is used to evaporate the refrigerant to saturated or superheated vapor *(1) -> (2)*. From the high pressure and temperature state at *(2)*, the fluid is expanded and mechanical work is produced *(2) -> (3)*. The low temperature heat sink *(5) -> (6)* cools the working fluid to saturated liquid at *(3) -> (4)*. At *(4)* the working fluid is pumped to the high-pressure level at *(1)* and thereby repeating the cycle.

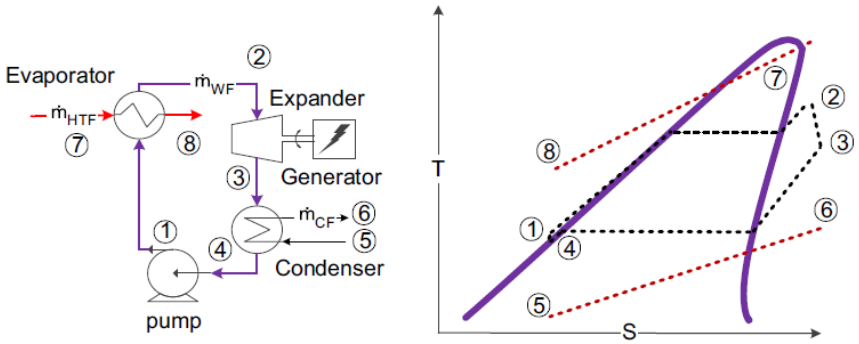

Figure 8. The basic ORC [12].

1.3.2.2 *Optimization*

Lecompte et al. [12] suggested in their review of ORC architectures for waste heat recovery important aspects when optimizing an ORC. Among these were, the working fluid of the ORC, the heat transfer process and the cycle configuration.

1. Heat transfer process

One important aspect when optimizing the ORC is to reduce the heat losses between the working fluid and the heat carrier. The heat carrier is the source which the ORC uses to evaporate the working fluid in order to expand it through the expander. It could be water or another fluid. Fig. 9 shows a temperature profile between the in and outlet temperature of a heat carrier and a working fluid in an evaporator. The grey area constitutes for the inability for the working fluid to absorb all the energy contained in the heat carrier. Due to a non-infinitely large heat exchanger, $\Delta T_{pinch\ point}$ is larger than zero and thereby increases the grey area in the diagram. Moreover, since the heat source is finite, the mass flow of the heat carrier will be limited and lead to an irreversible heat transfer loss in the upper grey area. The lower grey area constitutes for the heat loss from heat that remains in heat carrier after the evaporator.

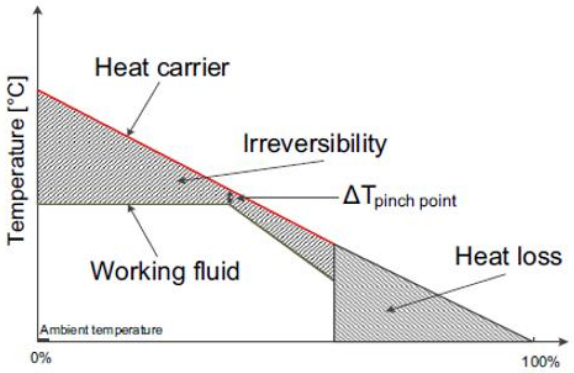

Figure 9. Losses between the heat carrier and the working fluid [12].

To reduce these losses and to improve the efficiency of the system it is necessary to, as best as possible, match the temperature profiles between heat carrier and working fluid.

2. Cycle Improvements – Matching the temperature profile

Following cycles are examples of improvements made in order to match the temperature profile between the working fluid and the heat carrier.

a) Transcritical cycle

In a transcritical cycle, evaporation is avoided by pumping the fluid to a pressure above its critical point. In Fig. 10**,** it can be seen that the temperature profile between the working fluid and the heat carrier better matches each other than the temperature profiles for the basic ORC in Fig. 8. Lecompte et al. [12] showed that while transcritical cycles can improve the work output it is on the expense of lower thermal efficiency.

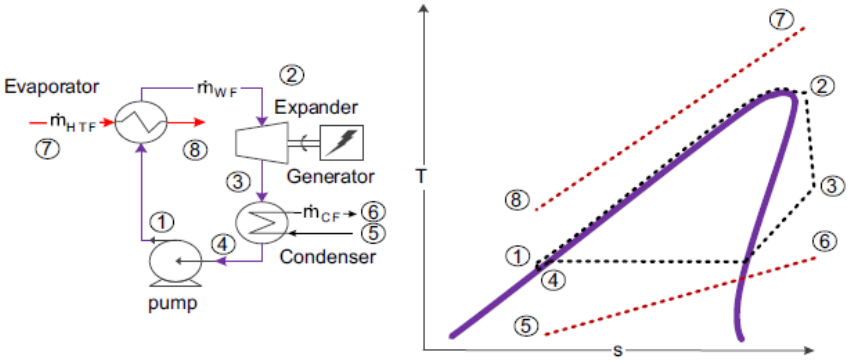

Figure 10. Transcritical ORC [12].

b) Trilateral cycle

The trilateral cycle has high potential to recover heat since the temperature profile between the working fluid and the heat carrier matches closely. Trilateral cycles avoid evaporation and the expansion takes place in the two-phase region. However, special expanders are required which are designed to work in the two-phase region in order to avoid erosion of the expander due to liquid droplets [12]. Li et al. [13] showed that trilateral cycle performs better in important efficiency parameters such as thermal efficiency, net power, exergy efficacy, in comparison to the basic ORC. An example of a trilateral cycle is shown in Fig. 11.

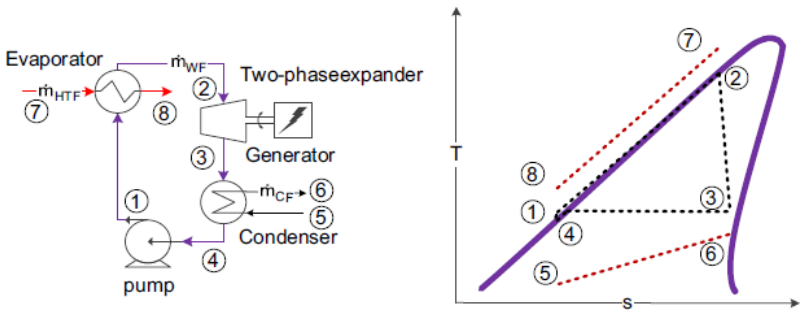

Figure 11. Trilateral ORC [12].

c) Cycle with Zeotropic mixtures

Another way of matching the temperature profiles is by using zeotropic mixtures. Since the fluids in a zeotropic mixture have different boiling points, there will be a slight increase in temperature during evaporation and a decrease during condensation. This makes the slope of the temperature curves more similar and thereby has the potential to decrease losses. Dong et al. [14] showed that ORC with zeotropic mixtures can produce more net power. However, it was also shown that larger heat exchangers were necessary which have unfavorable economic implications. Fig. 12 shows the schematic and T-s diagram of a zeotropic fluid used in an ORC.

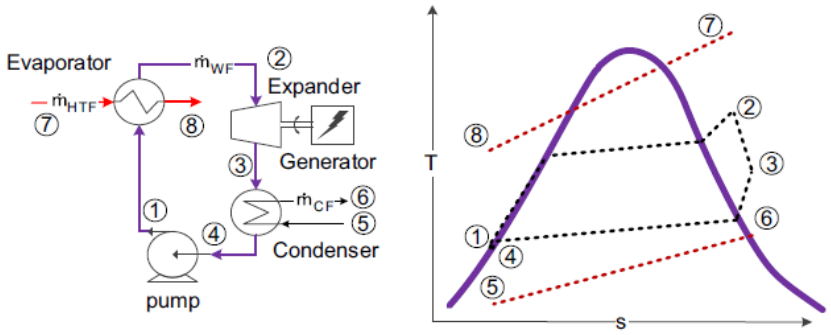

Figure 12. ORC using a zeotropic fluid [12].

3. Cycle Improvements – Maximizing the mean temperature difference

Another measure to increase the efficiency of the system is to maximize the temperature difference between the added and rejected heat [12]. One way of doing this is to reduce the condenser and evaporation load by using preheating.

a) Recuperating cycle

The recuperating ORC has a heat exchanger, a recuperator, which uses the superheated vapor at the expansion outlet to preheat the subcooled liquid before the evaporator. By doing this, the load on the condenser can be reduced as well as the load of the evaporator hence increasing the thermal efficiency. Fig. 13 shows the schematics of a recuperating cycle together with its corresponding T-s diagram. An ORC with recuperating is commonly used in many applications.

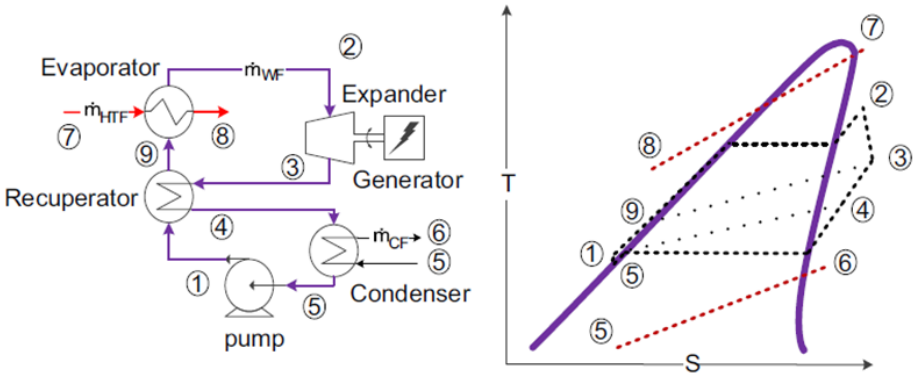

Figure 13. Recuperating ORC [12].

b) Regenerative cycle

In a regenerative cycle, a portion of the vapor is extracted from the expander to preheat the subcooled liquid coming from the condenser. The two streams mix and the outlet of the feedwater preheater is saturated liquid. The saturated liquid is then pumped to the evaporator. Although the loss of mass flow reduces the work output in the final stage expansion, the overall thermal efficiency will oftentimes be higher for the regenerative cycle than for the basic ORC [12]. Moreover, a combination of regenerative and recuperating systems can lead to even higher thermal efficiencies [15]. Fig. 14 shows the schematics of a regenerative cycle with its corresponding T-s diagram.

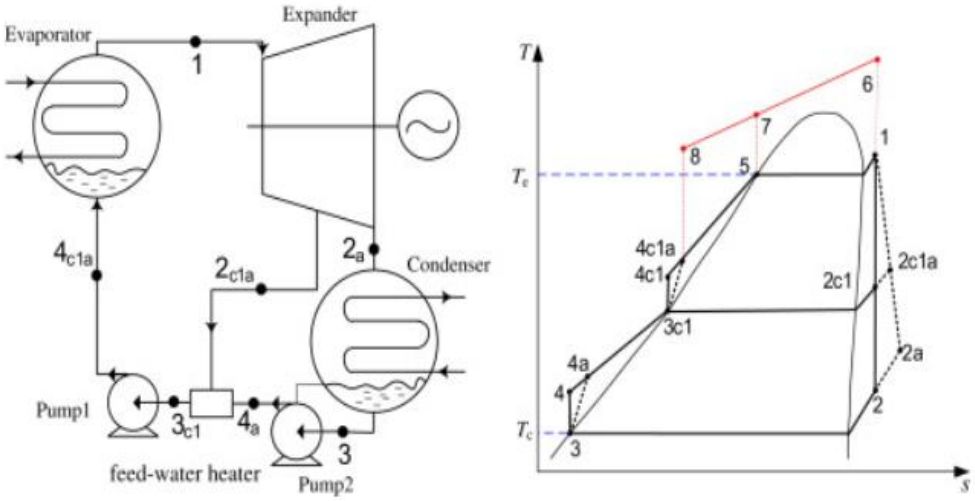

Figure 14. Regenerative ORC [16].

1.3.3 Selection of working fluid

The working fluid is an important parameter when analyzing an ORC and a HP. Nouman [17] suggested following desirable fluid characteristics:

- Critical pressure and temperature in the proper range for the application.
- The low-pressure level should be kept higher than atmospheric pressure to avoid suction of air in to the system.
- Low specific volume is preferable to keep the component size small and thereby the cost.
- High specific heat leads to better energy recovery.
- Low Global Warming Potential (GWP), low Ozone Depleting Potential (ODP), low toxicity and low flammability.

Another important characteristic of the working fluid is the curvature of the saturated vapor line. In Fig. 15, three different types of fluids can be identified. Wet fluids *(a)* have a negative slope of the vapor saturation line, dry fluids (b) have a positive slope and isentropic fluids *(c)* has a vertical (or close to vertical) slope.

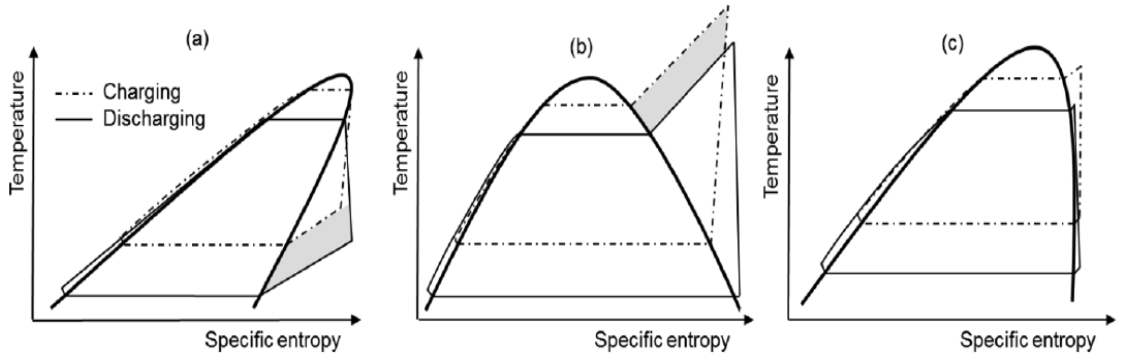

Figure 15. T-s diagram showing a charging and discharging cycle for three different types of fluids (a-dry, b-wet and c-isentropic) [18].

Fig. 15 also shows a HP cycle (charging) and an ORC (discharging) similar to the idea of the CHESTER system. The implications for each type fluid can be described as follows:

- Dry fluids
  - The work output in the ORC will be reduced due to a large degree of superheat at the turbine exit [19]. Groniewsky [20] points out that the large degree of superheat will increase the load of the condenser. A recuperator is therefore suggested in order to cool the superheated vapor to preheat the liquid before the evaporator.
  - A high degree of superheat is needed in the HP in order to avoid wet compression.
- Wet fluids
  - It is preferable to have a degree of superheating in the ORC before the expansion. If the working fluid would be expanded as saturated vapor, liquid formation in the two-phase region can cause erosion of the blades [20].
  - It is often necessary to include a multi-stage HP with intercooling to avoid high discharge temperatures.
- Isentropic fluids avoid the problems with dry and wet fluids. However, most isentropic fluids have a low critical temperature

1.3.4 Storage System

As explained in section 1.3.2.2, heat carrier and the working fluid should have similar temperature profiles in order to maximize the heat exchange. In the case for the CHESTER system, the storage system will be the heat carrier (or the source of evaporation) of the ORC. The storage system will also be used as condensation for the HP. The working fluid and the storage system should therefore have matching temperature profiles for both the ORC and the HP to maximize the efficiency. To achieve similar temperature profiles two types of heat storage can be used.

1. **Sensible heat storage**

In order to operate the system efficiently, the working fluid needs to be subcooled after it has condensated in the HP. This released energy during subcooling can be stored in a SHS (SHS) and later be used to preheat the working fluid for the ORC. A SHS uses the materials specific heat capacity to store energy and the total stored energy is a function of the specific heat, mass and the raise in temperature. There are different materials that can be suitable such as water, thermal oils, molten salts, concrete, liquid metals or different earth materials.

2. **Latent heat storage**

For the condensation in the HP and for the evaporation in the ORC, it would be more suitable to use LHS (LHS). In contrast to the material in a SHS, the material in a LHS unit undergoes a phase change when it is heated from a temperature below to a temperature above its melting temperature. This also occur during cooling and therefore the temperature profile between the evaporation in the ORC and the melting temperature will be similar. The most important characteristic of a material used in an LHS is its specific latent heat. The stored energy is a function of the specific latent heat as well as the mass. Suitable materials can be organic such as paraffin, fatty acids, esters, alcohols and inorganic materials such as salts and metals. [21]

1.3.5 Full System

Steinmann [22] investigated a concept similar to the CHEST system. Steinmann used a two separate cycles in order to raise the quality of the low temperature heat source. The source is used to evaporate ammonia which is later condensed in an intermediate heat exchanger. In the second stage cycle, water is evaporated from the latent heat released by the condensation of ammonia. The water is later condensed in a storage unit. Due to waters high specific volume at low pressures, which would generate a high volumetric flowrate, ammonia was chosen as the refrigerant for the lower temperature cycle. Ammonia is evaporated at 10.5 °C and the steam is condensed at 314.5 °C. Fig. 16 shows the basic layout of the charging system with corresponding Temperature-Entropy (T-s) diagram.

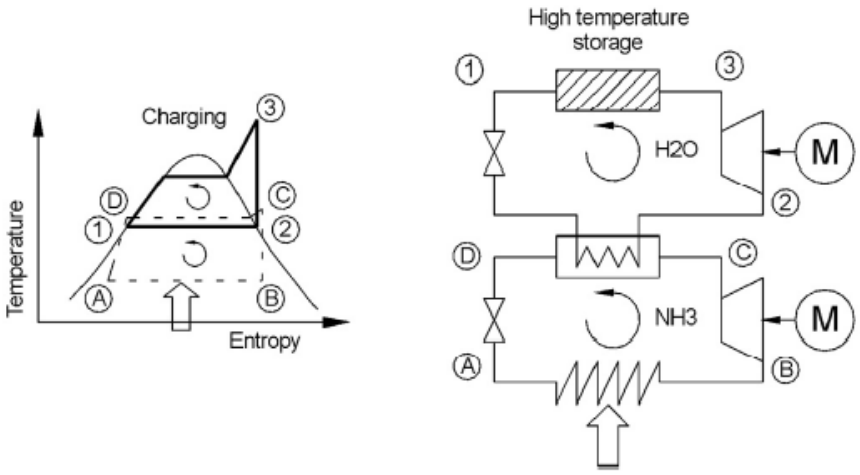

Figure 16. Layout of the charging cycle [22].

Fig. 17 shows a schematic of the complete charging-discharging system. One storage unit is used for latent heat and two units are used for sensible heat. By including both sensible and latent storage units, thereby matching the temperature profiles between the working fluid and storage units, the losses can be reduced. In this system, the superheated and subcooled regions of the working fluid is used to raise the temperature of the SHS and the condensing region is used to melt the PCM in the SHS units.

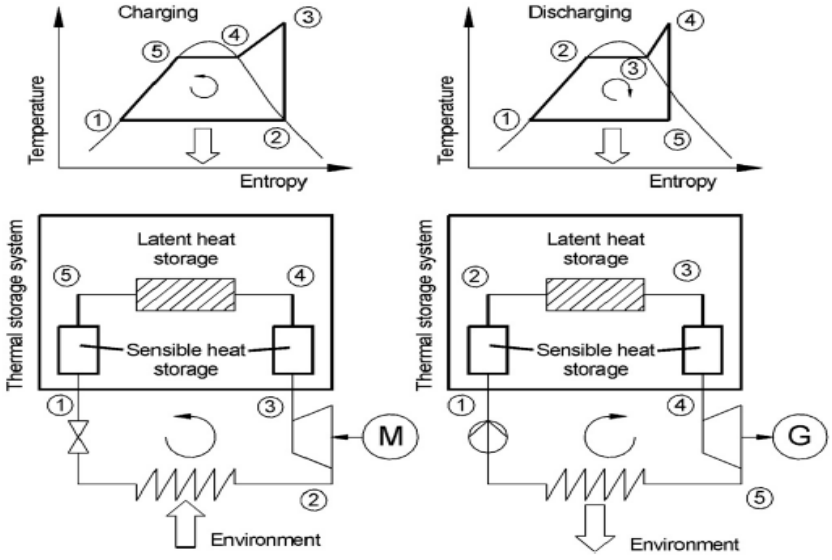

Figure 17. Layout of the discharging cycle [22].

Fig. 18 shows the discharging cycle. A conventional water-steam Rankine cycle with reheat is used to discharge the storage units. The low temperature sensible heat units raise the water temperature to saturated vapor conditions. In the LHS, the working fluid is evaporated at a temperature difference of 10 K from the phase change temperature of the PCM (305 °C). The high temperature SHS is used to superheat the steam just before it enters the first expansion.

After the first expansion, vapor and liquid are separated. The LHS reheats the vapor which is then expanded in the second stage turbine while the liquid returns to the low temperature SHS.

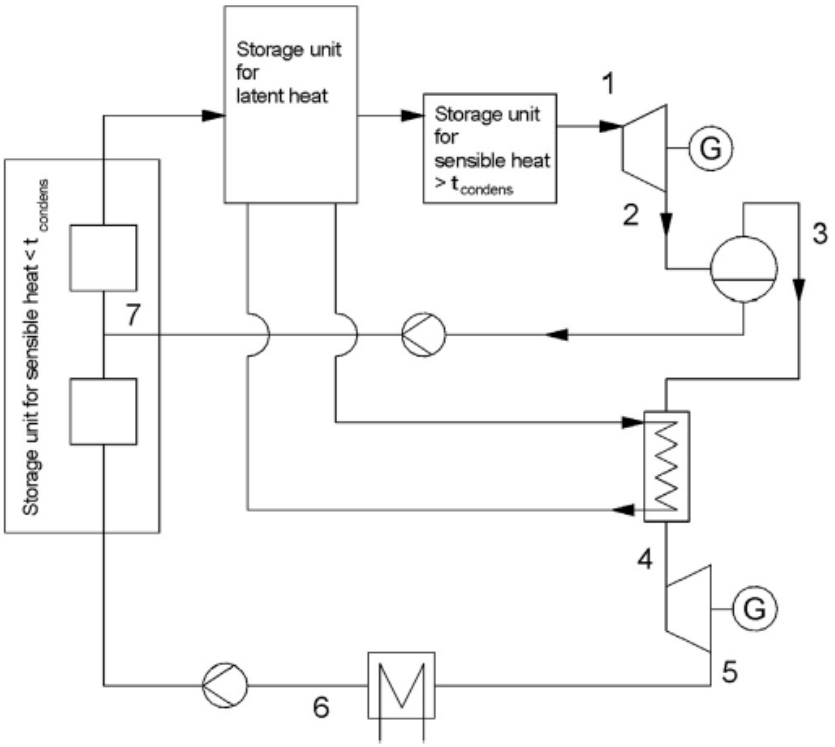

Figure 18. Schematic of the discharging system [22].

Steinmann showed that it is possible to reach a round trip efficiency ($W_{discharge}/W_{charge}$) higher than 1 if evaporation temperature is equal to or higher than 88°C, when condensation temperature is set to 27 °C.

Jockenhofter et al. [18] investigated a concept similar to Steinmann. The major difference from Steinmann is that the high temperature SHS was removed and the PCM replaced with another material with lower melting point (133 °C). Moreover, Jockenhofter et al. [18] used butene for both the charging and discharging cycle, making the discharging cycle an ORC. In Fig. 19, a schematic of the system is shown together with the corresponding T-s diagram. A one-stage heat pump cycle is used to charge the heat storage units. The working fluid condensates in the LHS and the PCM is melting. Thereafter, the sensible heat unit pumps the storage fluids through a counter current flow heat exchanger that transfer the heat between the working and storage fluid. The process is later reversed in the discharging cycle and electricity is generated.

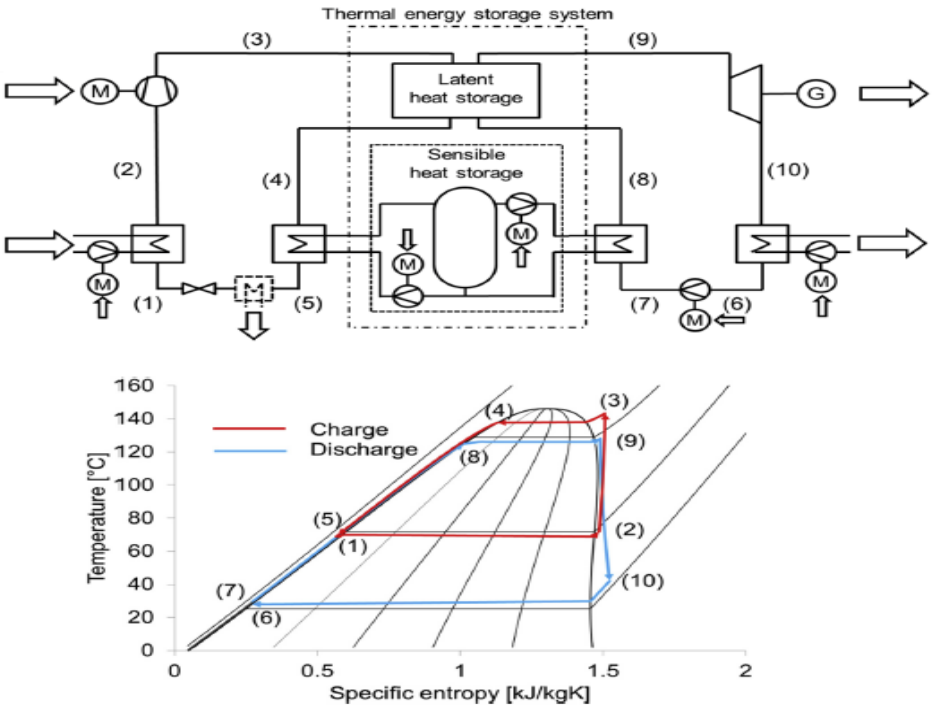

Figure 19. Schematic of the complete charging/discharging cycle [18].

Fig. 20 shows some of the results of the study. The gross roundtrip efficiency (ε_{gross}) is defined the electrical output of the expander during discharge, divided by the electrical input of the compressor during charging. The net round trip efficiency (ε_{net}), takes into account the electrical input to the auxiliary components (e.g. pumps) and is therefore lower than ε_{gross}, for the same boundary conditions. ε_{net} and ε_{gross} was plotted as a function of source temperature for two different sink temperatures. 5 K is used as the temperature difference between the working fluid and the source, storage and sink temperatures. It can be clearly seen from the figure that for a given sink temperatures, the roundtrip efficiency increases when increasing the source temperature.

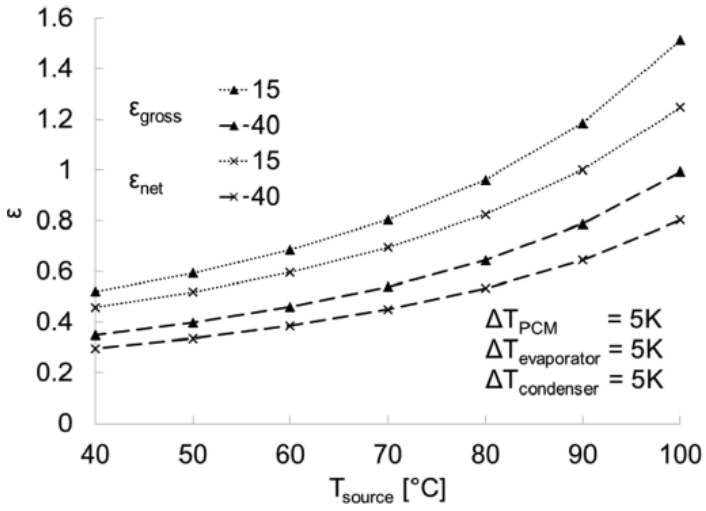

Figure 20. Gross and net roundtrip efficiency of the system [18].

2. METHODOLOGY

The methodology used in the project is explained in this section. The section explains the main equations used and schematics of the system. To see more detailed calculations and the values of the parameters used, please see appendix.

2.1 OVERALL SYSTEM (CHEST)

In Fig. 21 a basic layout of the overall system is shown. In the left cycle, the compressor uses excess electricity to pump the heat from lower temperature source to the high temperature TES system. This system comprises LHS (in which the desuperheating and condensation processes take place) and SHS (in which the working fluid is subcooled), respectively. Sometimes, several compression stages are needed to reduce the compression ratio and discharge temperature. After the sensible storage unit, the fluid is throttled down to evaporating pressure and the cycle is repeated. During times when there is a high electricity demand, the working fluid in the ORC is firstly preheated in the SHS, then evaporated and superheated in the latent heated heat storage unit. Secondly, it expands through the expander to generate electricity. Thirdly, it is condensed at a temperature slightly higher than the ambient sink temperature. Finally, it is pumped to the high-pressure level and the discharging cycle is repeated. For all the heat exchangers used, there is an assumed pressure drop of 5%.

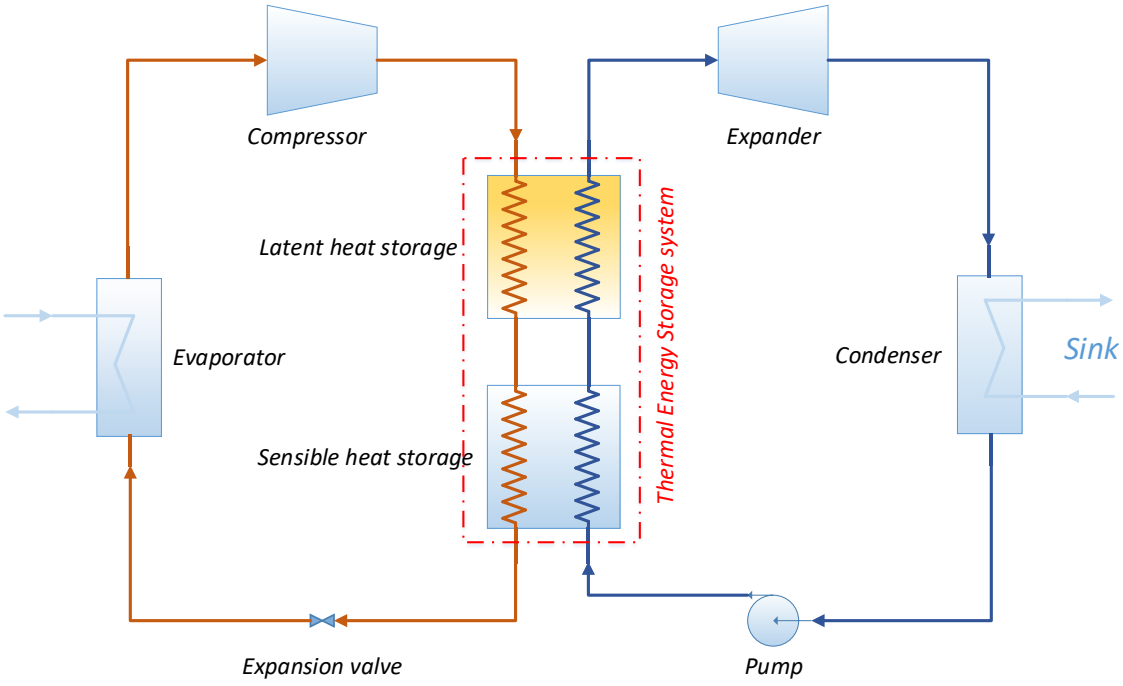

Figure 21. Layout of the overall system.

2.1.1 Performance indicators

The general equation used to assess the system efficiency is Eq. 1 where η_{round} is the mechanical roundtrip efficiency between the work output of the expander and work input by the compressor.

$$\eta_{round} = \frac{W_{expander}}{W_{compressor}} \quad (1)$$

2.2 Heat Pump Configuration

For different boundary conditions, the temperature lift will be different. As explained in the introduction, intermediate pressure levels can reduce the discharge temperature, reduce the total compressor work and increase the evaporation capacity. In the proposed, there is a possibility to introduce intermediate pressure levels. However, since different fluids have different properties the number of compression stages has been selected taking into account the performance parameters described in section 1.3.3.

Fig. 22 shows a detailed configuration of the heat pump and its connection to the storage system. When the number of compression stages have been selected, the number of flash tanks, compressors and SHS units change accordingly.

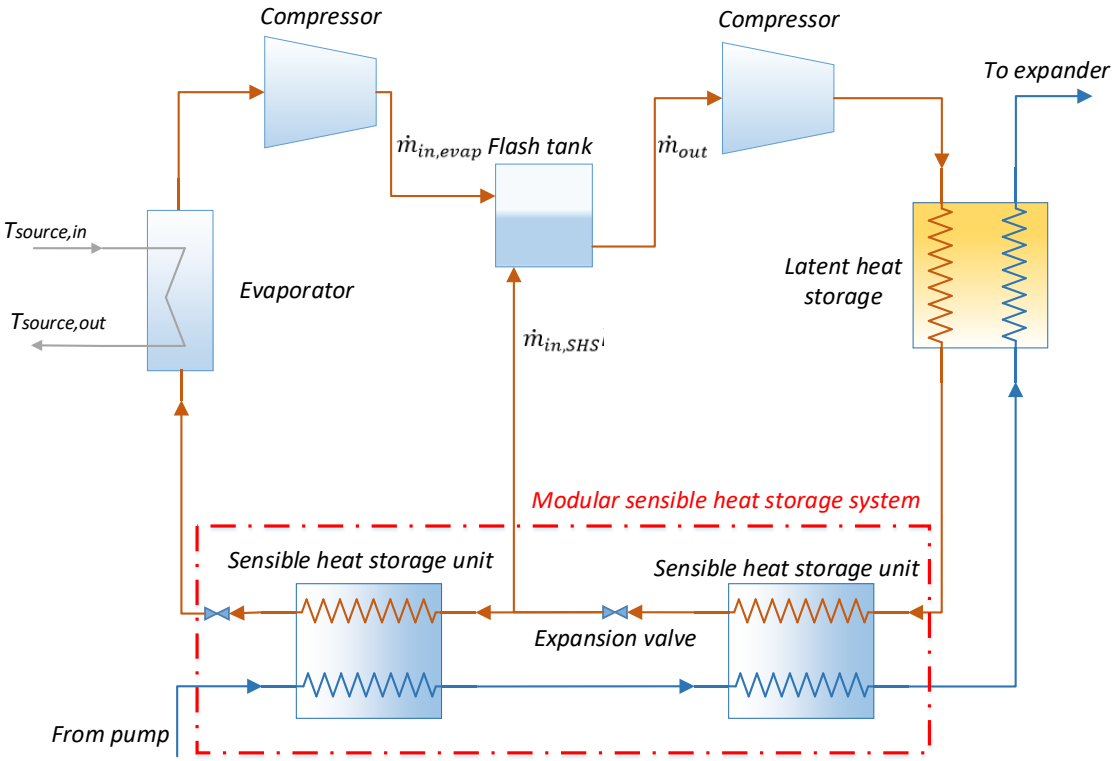

Figure 22. Configuration of the charging cycle.

The heat from the low temperature heat source is pumped into the evaporator where the working fluid is evaporated and, in some cases, superheated before entering the first compression stage. If there is at least one intermediate pressure level, the working fluid is cooled until saturated conditions by the condensate injected after the expansion valve between the SHS units.

2.2.1 Governing equations

For times when there are several compression stages, Eq. 2 [6] is used to obtain the optimum intermediate pressure (assuming similar pressure ratios between stages).

$$P_j = P_{evap}\left(\frac{P_{cond}}{P_{evap}}\right)^{\frac{i}{NSC}} \tag{2}$$

where *j* is the index for current intermediate pressure level, *P* is the pressure and *NSC* is total number of stages of compression.

The flash tank separates the superheated vapor and the two-phase flow that is coming from the extraction made after the SHS unit. Fig. 23 shows the energy balance over the tank and Eq. 3 shows the corresponding equation.

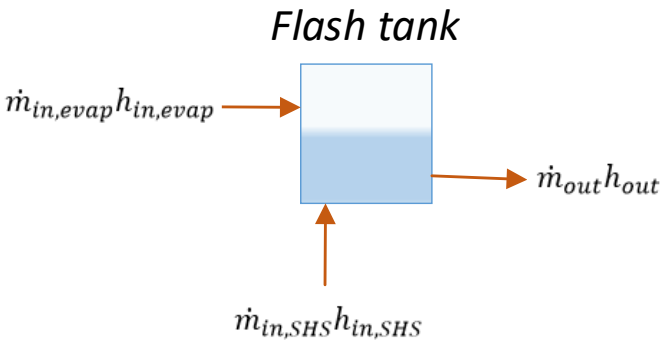

Figure 23. Energy Balance Flash Tank

$$\dot{m}_{out}h_{out} = \dot{m}_{in,SHS}h_{in,SHS} + \dot{m}_{in,evap}h_{in,evap} \tag{3}$$

Where $\dot{m}$ is the mass flow and *h* is the enthalpy. The isentropic compressor efficiency is assumed to be the same for all compressors and is calculated from Eq. 4

$$\eta_{comp} = \frac{h_{i+1,is} - h_i}{h_{i+1} - h_i} \tag{4}$$

Subscript i is dependent on how many compression stages are included in the model. After the final compression stage, the superheated fluid enters the LHS. The PCM material is now in solid form and starts to melt due to the heat transferred from the hot working fluid. The working fluid will cool down until it reaches the condensation temperature corresponding to the pressure at the outlet of the compressor. It leaves the LHS as saturated or subcooled liquid before it enters the SHS. The number of modular SHS units depends on the number of compression stages that are used in the cycle. To intercool between stages, a part of the subcooled liquid is drawn from the SHS units and injected just before the inlet of the intermediate compressors, as shown in Fig. 22.

2.2.2 Evaporator

The evaporator has been assumed to be a brazed plate counter flow heat exchanger that works under steady state condition. The pinch point approach has been adopted to size and analyze the thermal performance of the evaporator. Fig. 24 shows the temperature profiles of the refrigerant and water (which acts as the heat source), and location of pinch point and SH.

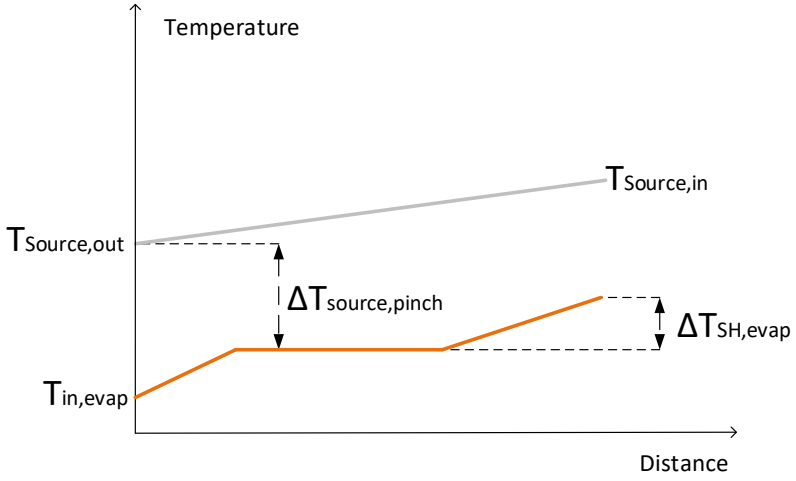

Figure 24. Temperature profile of the source heat exchanger.

2.2.3 Performance indicators

The Coefficient of Performance (COP) is the main performance indicator used for the HP. Eq. 5 shows how the COP of the heat pump is calculated.

$$COP_{HP} = \frac{\dot{Q}_{HP,tot}}{\dot{W}_{HP,tot}} \tag{5}$$

Where $\dot{Q}_{HP,tot}$ and $\dot{W}_{HP,tot}$ are the summation of the heat transferred to the storage units and the total power consumed by the HP, respectively.

The Volumetric Heat Capacity (VHC) is used to estimate the heat capacity per volume and it can be an indicator if the required compressor size. Equation 6 shows how the VHC is calculated.

$$VHC_{HP} = \frac{\dot{Q}_{HP,cond}}{\rho_1} \tag{6}$$

Where $\dot{Q}_{HP,cond}$ is the heat supplied to the LHS and ρ_1 is the density of the superheated vapor at the inlet of compressor.

Moreover, the lubrication oils need to be stable at the maximum temperature of the compressor. Therefore, the final discharge temperature $T_{discharge,final}$ will also be evaluated.

2.3 Organic Rankine Cycle

From the literature review, it was found that the regenerative-recuperative cycle has good potential to reach high efficiency at the same time as being reasonable complex. Many of the other cycles was considered to be either inefficient, too complex, or had a low degree of maturity. Therefore, the regenerative-recuperative cycle was considered an appropriate approximation of the real cycle.

Fig. 25 shows the cycle layout of the ORC cycle coupled with the storage system. Depending on the number of compressor stages in the heat pump, there will be one or several SHS units with different temperatures. The working fluid leaves the LHS as slightly superheated vapor before it is expanded to condensation pressure. The expansion consists of two pressure stages where a vapor extraction is made after the first stage and the vapor is fed to a flash tank. The recuperator is used to heat the subcooled fluid after the pump with the outlet superheated vapor from the expander. The outlet of the flash tank is saturated liquid which is pumped to high pressure at the inlet of the sensible heat units.

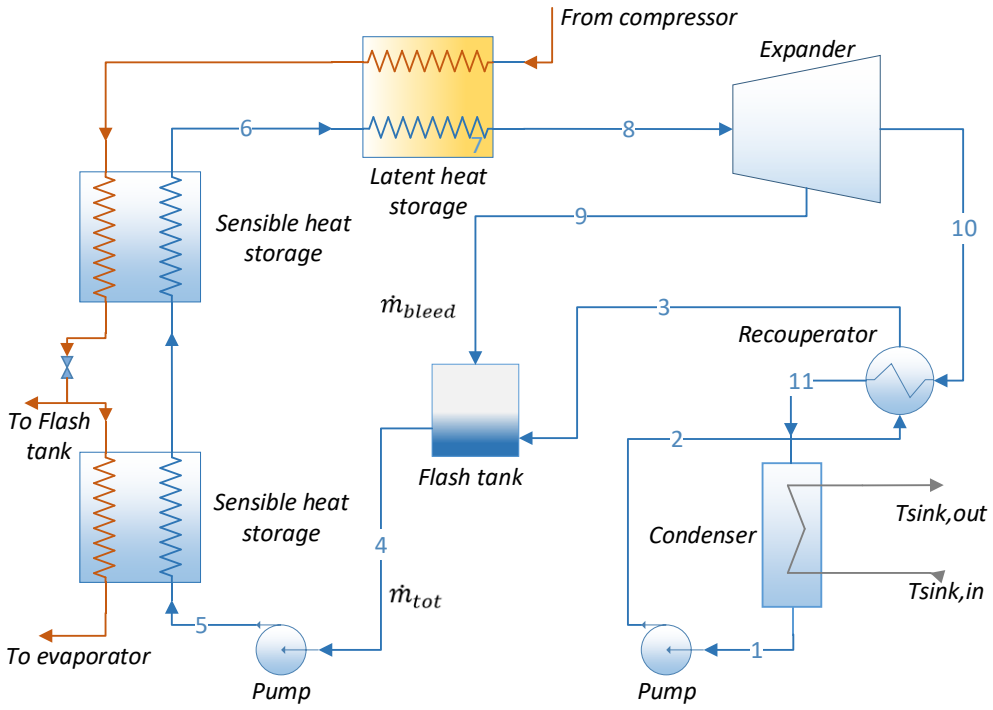

Figure 25. ORC with recuperator and regenerator.

2.3.1 Governing equations

Eq. 7 shows the energy balance over the regenerator

$$h_4 \dot{m}_{tot} = h_9 \dot{m}_{bleed} + h_3(\dot{m}_{tot} - \dot{m}_{bleed}) \tag{7}$$

By introducing x_{bleed} [23] as a function of the mass flow of the extraction of vapor from the expander and the total mass flow Eq. 8 gives

$$x_{bleed} = \frac{h_4 - h_3}{h_{11} - h_3} \tag{8}$$

Eq. 9 shows the energy balance over the recuperator

$$h_3 - h_2 = h_{10} - h_{11} \tag{9}$$

Eq. 10 shows the recuperator effectiveness and is defined as

$$\varepsilon_{rec} = \frac{h_3 - h_2}{h_{10} - h_{2,prim}} \tag{10}$$

Where $h_{2,prim}$ is the smallest enthalpy value that h_2 can have with the condition $T_{10} = T_2$.

Eq. 11 shows the isentropic efficiency of the pumps, which is calculated as

$$\eta_{pump} = \frac{h_{i+1,is} - h_i}{h_{i+1} - h_i} \tag{11}$$

Where *i* is 0 and 3.

Eq. 12 shows how the bleed pressure is defined.

$$P_{bleed} = P_i\left(P_{evap} - P_{cond}\right) + P_{cond} \tag{12}$$

Where P_i is a value from 0 to 1. This equation makes P_{bleed} vary between the condensation pressure (when $P_i = 0$) and the evaporation pressure (when $P_i = 1$).

2.3.2 Condenser

Fig. 26 shows the temperature profiles of the refrigerant and water (which acts as heat sink), temperature differences and location of pinch point. Superheated vapor enters the condenser from the outlet of recuperator and is cooled until saturated vapor conditions. Thereafter, it is condensed till the saturated liquid conditions where it reaches the pump. The distance in the graph should not be mistaken for a real scale and is only used to clearly represent the temperature profiles in the unit.

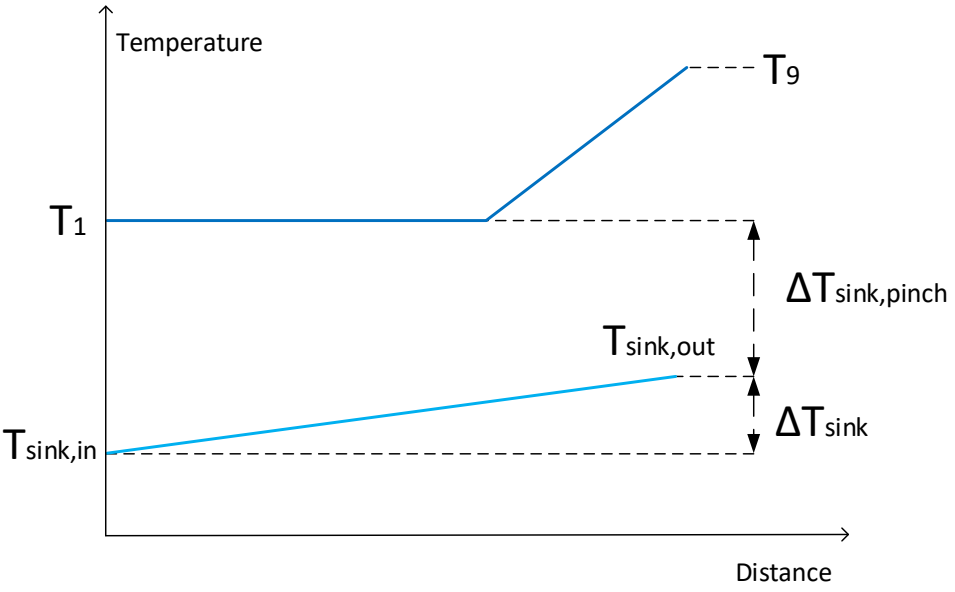

Figure 26. Temperature profile in the sink heat exchanger.

2.3.3 Performance indicators

Following parameters are used to evaluate the system performance for the ORC. The thermal efficiency is defined in Eq. 13 as the work output of the expander divided by the total thermal input from the storage unit.

$$\eta_{thermal} = \frac{\dot{W}_{net}}{\dot{Q}_{in}} \tag{13}$$

In order to avoid supersonic flow problems, large sized expanders and a large number of stages, the specific volume ratio between the outlet and the inlet of the expander should be as low as possible. Therefore Rayegan et al. [24] suggested adding a parameter, VER (Vapour Expansion Ratio), to the evaluation, shown in Eq. 14

$$VER = \frac{v_{out}}{v_{in}} \tag{14}$$

2.4 Thermal Energy Storage Units

Fig. 27 shows a layout of the storage system. From the outlet of the compressor, the working fluid charges the latent and sensible storage units by the heat released from working fluid during condensation and subcooling processes. In case of many compression stages, a part of the liquid is drawn to the flash tank between the sensible storage units. After the last SHS unit, the working fluid returns to the evaporator and the process is repeated.

A high temperature SHS was not included because highly superheated vapor in the ORC was not considered to increase the performance of the system considerably without adding much more complexity.

During discharge, the ORC uses the same energy supported by the HP in order to heat and evaporate the working fluid. Firstly, the working fluid is preheated by pumping it to the SHS, which in case of multiple compression stages will have two or more units with different temperature levels. Then, the fluid is evaporated and superheated in the LHS till reaching the expander inlet.

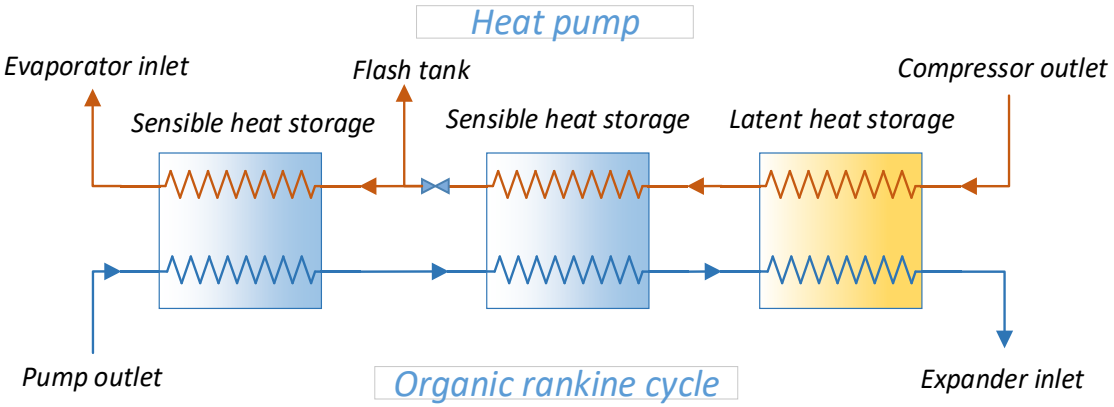

Figure 27. The thermal storage system.

2.4.1 Latent storage system

Although this work has not focused on the storage units, a short review was made in order to find possible materials for the LHS unit. The LHS unit contains a PCM that will undergo a phase change when the system is charging and discharging. For an efficient storage, the PCM should have high latent heat of fusion as well as specific heat and thermal conductivity [25]. To know the condensation and evaporation temperature of the HP and the ORC it is necessary to find materials that have a melting temperature in an appropriate range for the application. Table 1 shows the three selected materials that was used in the thermodynamic analysis of the CHEST system.

Table 1. Melting temperature of three selected PCMs.

Material	T_{melt} (°C)
$LiNO_3$–KNO_3 [26]	133
KNO_2-$NaNO_3$ [26]	149
LiOH-$LiNO_3$ [26]	183

Eq. 15 shows the relation between the latent heat supplied by the HP and the heat absorbed by the ORC. Independent of the boundary conditions, the ratio between the sensible heat supplied by the heat pump to the storage system and the sensible heat absorbed by the ORC is the same.

$$\dot{Q}_{HP,lat} = \dot{Q}_{ORC,lat} \tag{15}$$

Since the ORC will discharge at lower temperatures than the HP, there is a mismatch between the points of saturation between the ORC and the HP. Therefore, depending on the boundary conditions, the working fluid might not be saturated when it enters the inlet of the LHS during discharge. The temperature profiles in the LHS unit along with the defined temperature differences are shown in Fig. 28.

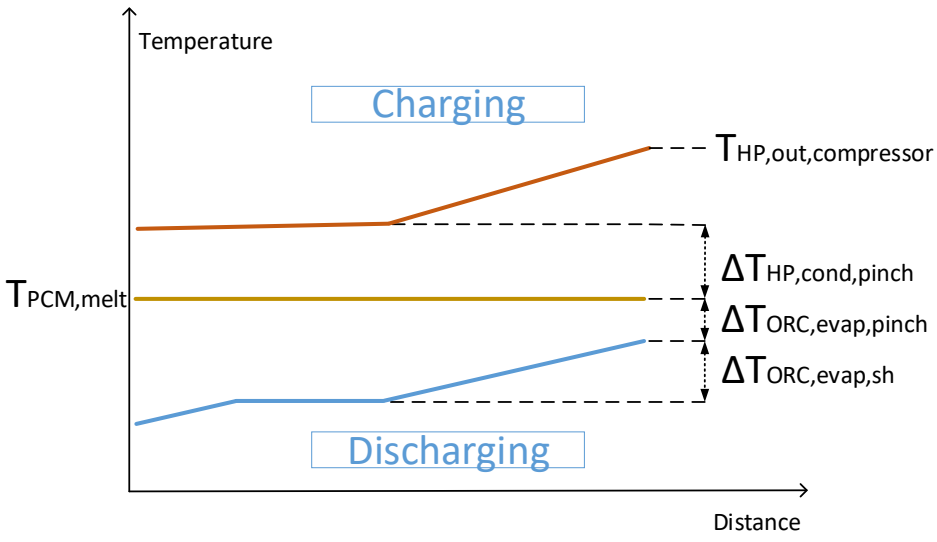

Figure 28. Temperature profile of the heat exchanger in the LHS.

2.4.2 Sensible heat storage

The SHS uses water as the storage medium. Fig. 29 shows the layout of one of the SHS units, if necessary, it is also possible to install two or more SHS units in series. During charging, the cold water in the Low-temperature water tank is pumped through a heat exchanger that transfers the heat from the subcooled working fluid in the HP. The hot water is pumped to the High-temperature water tank where it is stored. During discharging, the hot water is pumped to a heat exchanger which is used to preheat the working fluid in the ORC. The cold water is then stored in the Low-temperature water tank where it is kept until the next cycle.

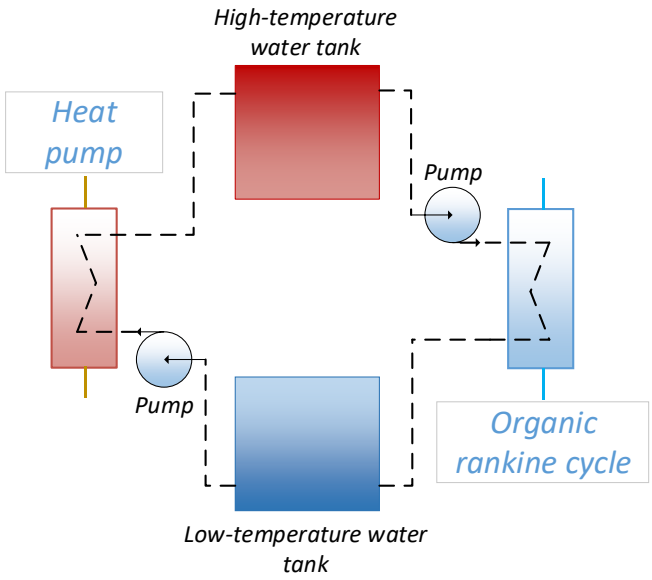

Figure 29. Schematic of the SHS.

The SHS system is assumed to transfer all the energy supplied by the HP to the ORC. This is shown in Eq. 16 where:

$$\dot{Q}_{HP,sens} = \dot{Q}_{ORC,sens} \tag{16}$$

The temperature profiles inside the SHS unit can be seen in Fig. 30. The black dotted line shows the approximated flow of water during charging and discharging. After the working fluid has left the LHS during charging, it will enter the SHS as saturated liquid. The temperature of the working fluid at the outlet of the SHS is determined by T_{LTWT} plus a temperature difference, $\Delta T_{w,pinch,SHS}$. For the discharging case, the temperature of the working fluid at the inlet of the SHS is determined from the outlet of the pump. At the outlet of the SHS, the temperature of the

working fluid is determined by T_{HTWT} minus $\Delta T_{w,pinch,SHS}$. $\Delta T_{w,SHS}$ is set as the highest input possible without any temperature crossing of the lines.

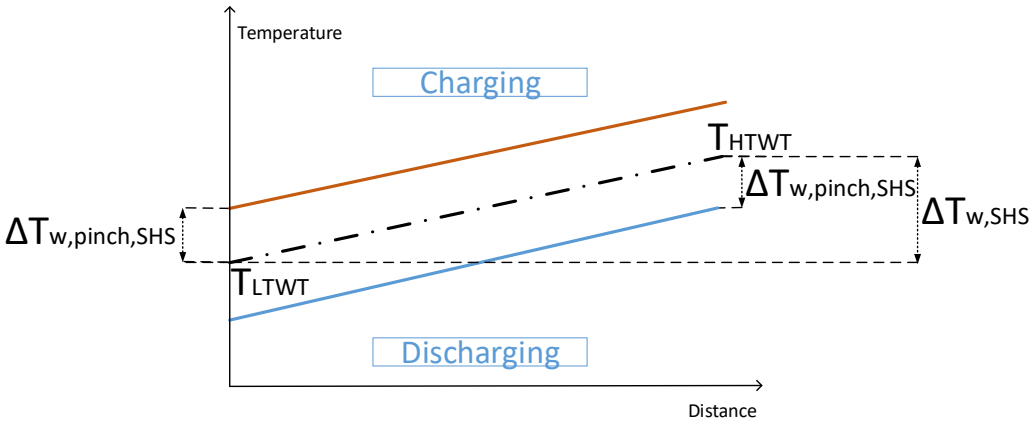

Figure 30. Temperature profile of the heat exchangers in the SHS.

2.5 Refrigerant Selection

Many different working fluids for a high temperature HP and ORC systems can be found in literature. As explained in the previous section, the boundary conditions for the specific application is one of the most important criteria when selecting a suitable refrigerant. The most common refrigerants found in literature are represented in the Table. 2. Based on the previous discussion in section 1.3.3, the working fluids are divided into three different categories depending on the slope of the saturated vapor curve on T-s diagram: dry fluids (orange), isentropic fluids (green), and wet fluids (blue). The sink temperature is expected to be similar to the ambient and therefore the saturation pressure has been calculated at 25 °C. The GWP-values are demonstrated when information is available.

Table 2. Selected refrigerants categorized by type, normal boiling point (NBP), critical temperature, pressure at 25 °C and critical pressure.

Refrigerant	Type	NBP (°C)	T_{crit} (°C)	$P_{25\,°C}$ (kPa)	P_{crit} (kPa)	GWP
Acetone [27]	Wet	56	235	31	4700	<1 [28]
Methanol[29]	Wet	64	240	17	8216	2.8 [28]
Ethanol [29]	Wet	78	242	8	6268	
R123 [30]	Isentropic	28	184	91	3662	77 [31]
R141b [30]	Isentropic	32	204	79	4212	725 [32]
Benzene [29]	Isentropic	80	289	13	4907	
Cyclohexane [24]	Isentropic	81	280	13	4081	
Dimethyl carbonate [29]	Isentropic	90	284	7	4909	
Toluene [24]	Isentropic	111	319	4	4126	
R1233zd (E) [33]	Isentropic	18	165	130	3573	Very low [34]
R1234ze (Z) [35]	Isentropic	10	150	179	3533	Very low [34]
Butene [18]	Isentropic	-6	146	297	4005	
R245fa [7]	Isentropic	15	154	148	3651	
HFO1336mzz (Z) [36]	Dry	33	171	100	2900	2 [36]
R601a [30]	Dry	28	187	92	3378	20 [30]
R601 [30]	Dry	36	197	68	3370	20 [30]
R365mfc [30]	Dry	40	187	57	3266	
R113 [23]	Dry	48	214	45	3392	4800 [37]
Cyclopentane [10]	Dry	49	239	42	4571	10 [38]
Isohexane [24]	Dry	60	225	28	3040	
Hexane [24]	Dry	69	235	20	3034	
Heptane [24]	Dry	98	267	6	2736	
Octane [24]	Dry	126	296	2	2497	
Nonane [24]	Dry	151	321	1	2281	
Decane [24]	Dry	174	345	<1	2103	

It can be seen that most refrigerants require a condensation pressure in the ORC below atmospheric. For some of the dry fluids the pressure needs to be very low for condensation to be possible. This will be problematic since the condenser is required to work with pressures below atmospheric, and therefore there is a risk of air infiltration into the system. In water-steam Rankine cycles, a deaerator uses injected superheated steam from the turbine to release any air in the system to the atmosphere. For ORC systems, this might not be possible due to environmental impacts, flammability, toxicity, or cost of the working fluids. A common method to solve this issue is to use a vacuum pump that removes a mixture of the refrigerant and air from the condenser and then flows through a carbon filter that absorbs the organic substance

[39]. Consequently, for condensation temperatures of 25 °C or lower a vacuum pump will have to be introduced to the system in order to remove possible air infiltration.

2.6 Case Study

Fig. 31 shows the working range for the fluids in Tabel 2. The working range is defined as the temperature difference between the normal boiling point and the critical temperature. The dotted red lines show the proposed sink temperature and 3 condensation temperatures in HP. These dotted lines are based on the selected PCM materials from Table 1. Since there is a pinch point difference between the PCM and the working fluid, 5 K has been added for each condensation temperature in the HP.

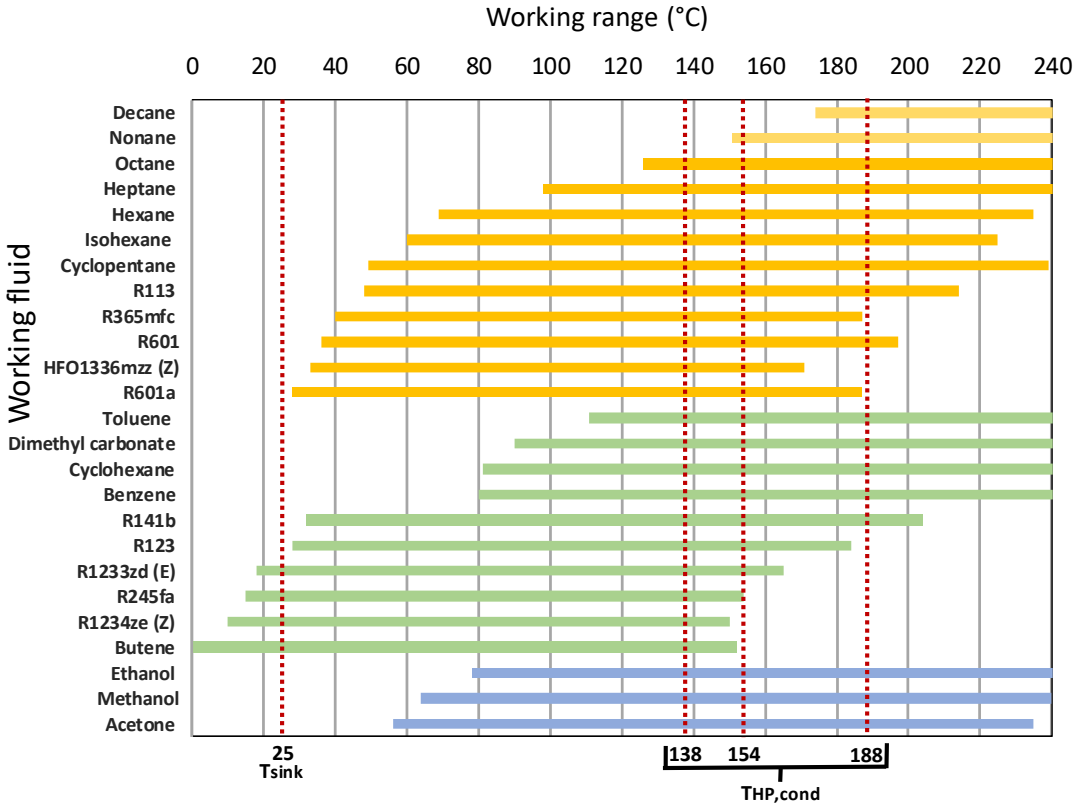

Figure 31. Working range of selected refrigerants.

To investigate the outcome of the different fluid categories (wet, dry or isentropic) one refrigerant of each category has been chosen.

2.6.1 Low temperature storage, Case 1

The first scenario was developed using $LiNO_3$–KNO_3 as the LHS material. The working range required for this scenario is from 25 to 138 °C. As a wet fluid, Acetone has been selected because it has the lowest natural boiling point of the wet fluids in the table. This means that the condenser of the ORC cycle has to work with a higher pressure than for Ethanol and Methanol. As an isentropic fluid, R1233zd(E) is in the required range and it also have a low GWP value. As a dry fluid HFO1336mzz(Z) has been selected due to its low natural boiling point as well as a low GWP value. Moreover it has low toxicity and low flammability which makes it a preferred option over for example R601a [36].

2.6.2 Medium temperature storage, Case 2

The working range required for this scenario is from 25 to 154 °C. The same refrigerants have been chosen for this scenario as for the low temperature storage.

2.6.3 High temperature storage, Case 3

The working range required for this scenario is from 25 to 188 °C. For the high temperature storage, Acetone has been selected as the wet fluid. R141b has a natural boiling point that is close to the sink temperature and it has a critical temperature above 188 °C. It is in fact the only isentropic refrigerant which has a natural boiling point close to the sink while it still has a sufficiently high critical temperature. Unfortunately, it has a high GWP value and therefore the system designer needs take measures in order to prevent leaking. With these considerations taken into account, it was chosen as best the isentropic fluid for the high temperature storage. As Cyclopentane is a common fluid to use in ORC system and has a neglectable GWP it was chosen as the dry fluid. A flammable, low GWP fluid has a natural boiling point that is higher than the sink temperature.

2.7 SIMULATING SOFTWARE

Engineering Equation Solver (EES) has been used to develop the proposed model for the CHEST system and to run the simulations and parametric studies. This program has been chosen because it allows for simple programing, direct access to the thermal properties of a vast amount of working fluids, and detailed output results and figures.

2.8 SAFETY VARIABLES

In order to prevent crossings of temperature profiles in the heat exchangers, violating the second law of thermodynamics, and wet compression, it is necessary to include a number of constraints in the model called safety variables. The safety variables of the system are explained in Table 3.

Table 3. Safety variables

Safety Variable	Safety Variable	Condition
ϕ_1>0 [kJ/kg]	Prevent wet compression	$h_{HP,comp,out}$-$h_{HP,sat}$
ϕ_2>3 [°K]	Temperature outlet of LHS	$T_{HP,lat,out}$-T_{melt}
ϕ_3>3 [°K]	SHS bottom temperature	T_{LTWT}-$T_{ORC,pump,out}$
ϕ_4>3 [°K]	SHS top temperature	T_{HTWT}-$T_{HP,lat,out}$
ϕ_5>3 [°K]	Evaporation outlet temperature	$T_{source,in}$-$T_{HP,evap,out}$

To fulfill the conditions for the safety variables is very important in order to not brake any thermodynamic laws during the simulation. This part of the methodology can be seen in the flowchart in Fig. 32. The program moving to the next step of the simulation if the conditions of the safety variables in Tabel 3 is true.

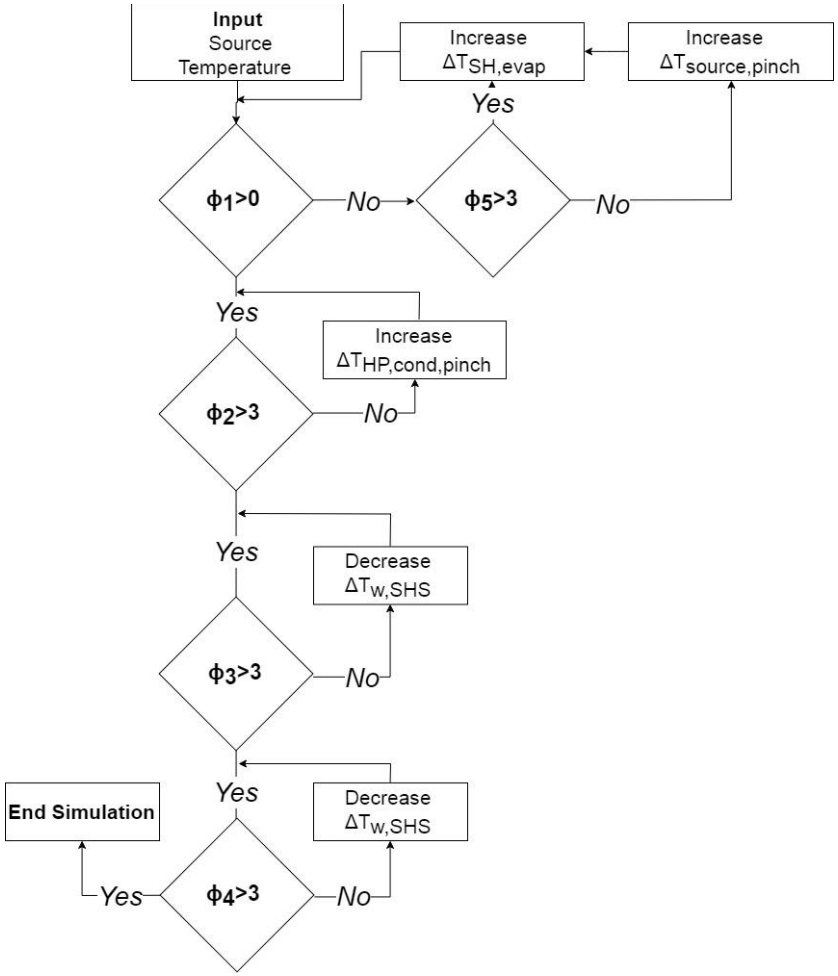

Figure 32. Flow Chart for simulation of safety variables.

3. RESULTS AND DISCUSSION

3.1 CASE STUDY BASED ON PCM MELTING TEMPERATURE

The first part of the results section will include the simulations of the CHEST system for three cases regarding the PCM melting temperatures in Table 1 and suggested refrigerants for each case. The HP has been selected to use one stage compression for all the refrigerants except for Acetone where two-stage compression are included in the analysis. In the initial analysis, the ORC has been set to be a simple cycle without recuperation or regeneration. The performance indicators explained in the methodology have been calculated by varying the source temperature from 40 to 100 °C. The sink temperature is kept constant as 25 °C. The pressure drop is kept constant at 5% for all heat exchanger and the pinch point temperatures are kept at 3 K.

In the second part of the results a more detailed analysis is done using the R1233zd(E) as working fluid in the system, in order to evaluate the impacts of pressure drop variation in the heat exchangers, pinch points variation, recuperation and regeneration processes on the whole CHEST system performance.

3.1.1 Case 1 (T_{melt}=133 °C)

The selected refrigaerants that is used for comparison in this case is Acetone, R1233zd(E) and HFO1336mzz(Z).

a) Cycle simulation on T-s diagram

Fig. 33 shows the T-s diagram of the system for the three selected working fluids, where the source temperature was set to 70 °C an average between 40 and 100 °C. The red line represents the HP cycle while the blue one represents the ORC. It can be clearly noticed the difference in the slope of the saturated vapor line and the effect of the evaporation temperature. Since the dry fluid, HFO1336mzz(Z), has a positive saturation curve, a high degree of superheating is needed which will make the evaporation temperature much lower. This will reduce significantly the COP of HP cycle. Moreover, for the expansion case it is clear that the degree of desuperheating in the ORC's condenser is very high. In contrast to HFO1336mzz(Z), Acetone is highly superheated after the compression. Since the compression efficiency is assumed to the be the same for all fluids, the negative slope of the vapor saturation curve causes high superheat after compression. R1233zd(E) is considered an isentropic fluid but since the slope is slightly dry a small amount of superheat at the outlet of HP's evaporator is needed, in order to prevent the wet compression.

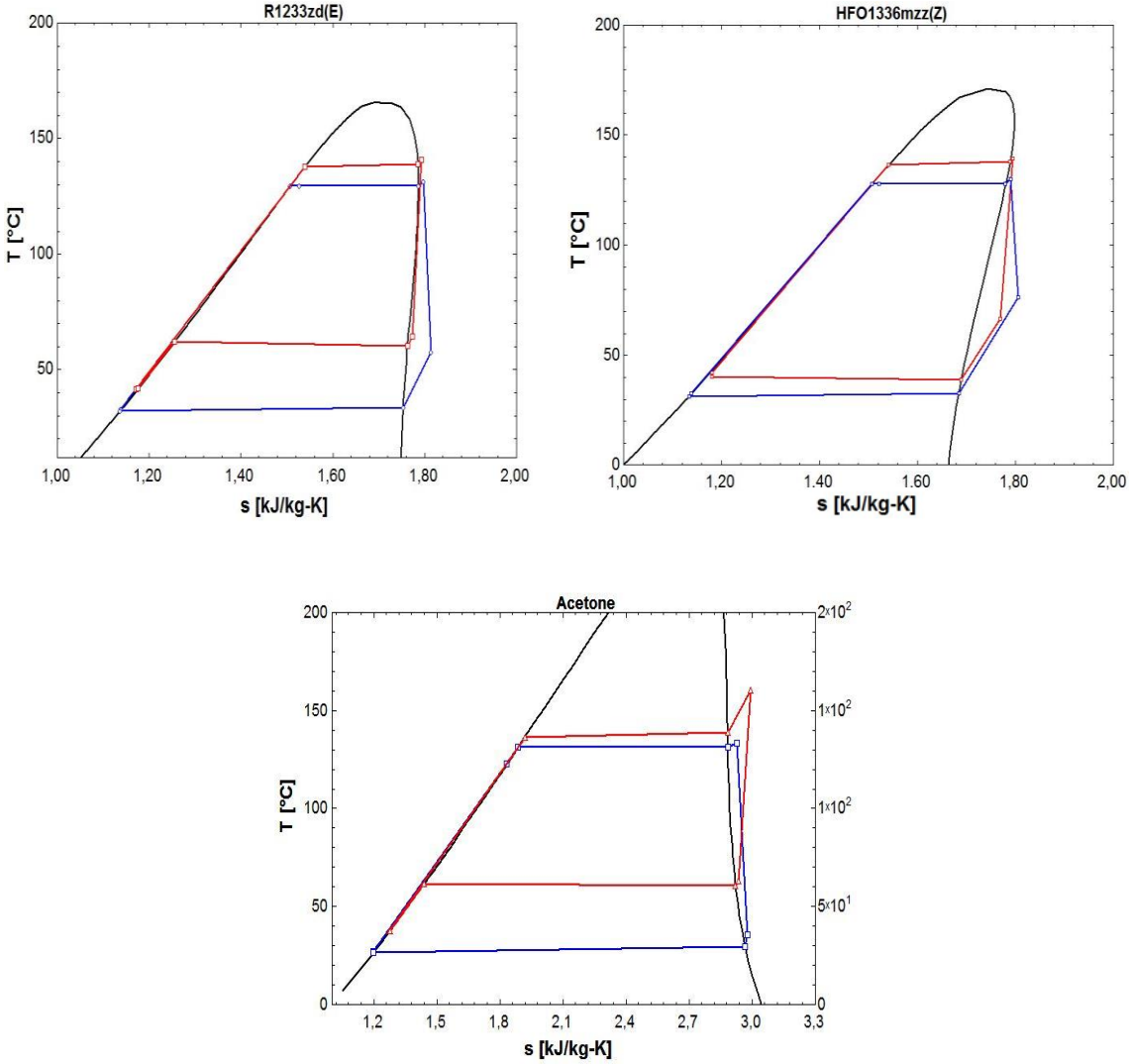

Figure 33. Cycle representation on T-s diagram for the working fluids used in Case 1, where T_{source}=70 °C.

b) Overall system performance

Fig. 34 shows the roundtrip efficiency as a function of source temperature for the three selected refrigerants in Case 1. For all the refrigerants, the general trend when increasing the source temperature is an exponential increase of the roundtrip efficiency. When comparing the refrigerants, the roundtrip efficiency for Acetone (one and two stage) and R1233zd(E) are very similar and reach a roundtrip efficiency of 1 at T_{source}=75 °C. For HFO1336mzz(Z), the roundtrip efficiency is lower for the whole range and a roundtrip efficiency of one is reached at T_{source}=87 °C. The roundtrip efficiency is lower for the dry fluid because the degree of superheating is higher.

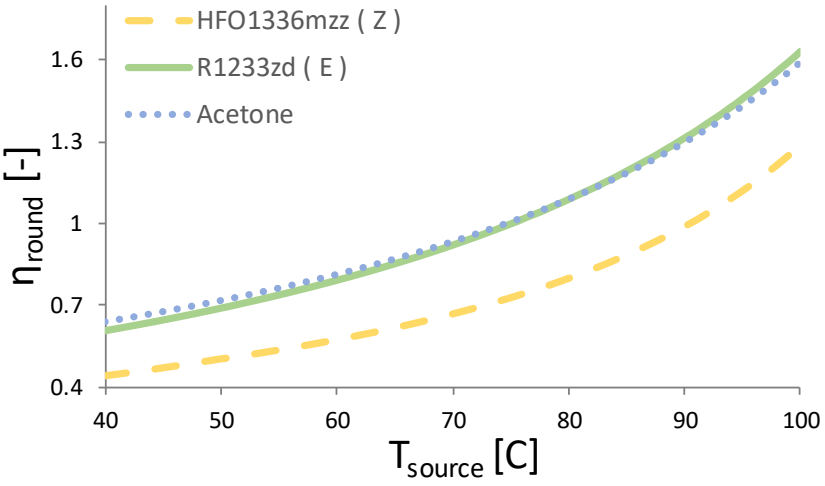

Figure 34. Roundtrip efficiency for CHEST system for Case 1.

c) Heat pump cycle performance

As explained in the methodology, the VHC can be used as a prediction of the compressor size based on the required heat that is supplied to the heat storage system. Fig. 35 shows the VHC as a function of source temperature. At low source temperatures, Acetone has very good VHC, which would require a small compressor size compared to other refrigerants. The VHC for Acetone decreases with the increase of source temperature. However, at 100 °C it is still about 20 times higher than the other working fluids. HFO1336mzz(Z) has a slightly better VHC for 40 °C < T_{source} < 70 °C.

Fig. 36 shows the final discharge temperature versus the source temperature. As expected from a wet fluid, Acetone has the highest discharge temperature which can damage the compressor and affect the thermal properties of the lubrication system. The final discharge temperature for Acetone reaches 176 °C when T_{source} is 40 °C. As T_{source} is increased the final discharge temperature is reduced and reaches 150 °C when T_{source}=100 °C. The discharge temperature for HFO1336mzz(Z) is kept constant at saturated vapor conditions in order to prevent wet expansion. As R1233zd(E) has a saturated vapor line which turns slightly dry for higher temperature, the discharge temperature increases when the source temperature is higher than 70 °C.

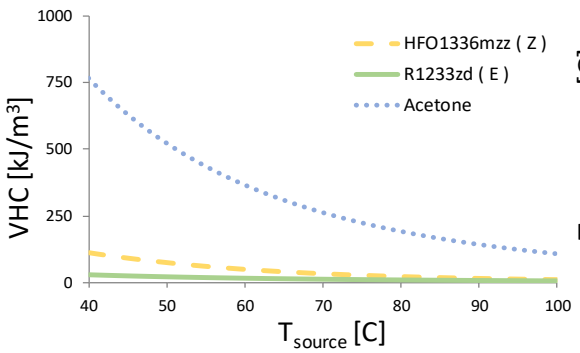

Figure 35. HP volumetric heating capacity, Case 1.

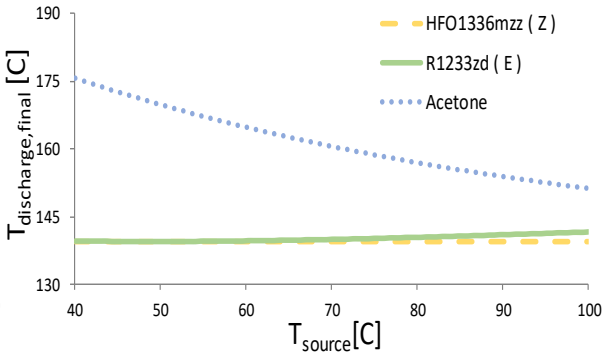

Figure 36. HP final discharge temperature, Case 1.

Fig. 37 shows the COP_{HP} as a function of the source temperature. In accordance with the Carnot efficiency, the COP_{HP} will be higher when the temperature lift is smaller. R1233zd(E) has the highest COP_{HP} which is 11.5 when T_{source}=100 °C. Since it is an isentropic fluid, the compressor work is the smallest compared to other two fluids which also can be concluded from Fig. 33.

The degree of superheating employed can be seen in Fig. 38. A very high degree of superheat is needed for HFO1336mzz(Z) in order to prevent wet compression. When T_{source}=40 °C, a superheat of 30 K is required in order to avoid wet compression. When T_{source}=100 °C, a superheat of 16 K is necessary. R1233zd(E) and Acetone require very low superheat for the whole temperature range. Superheat has a large effect on the roundtrip efficiency since evaporation temperature will downgrade substantially.

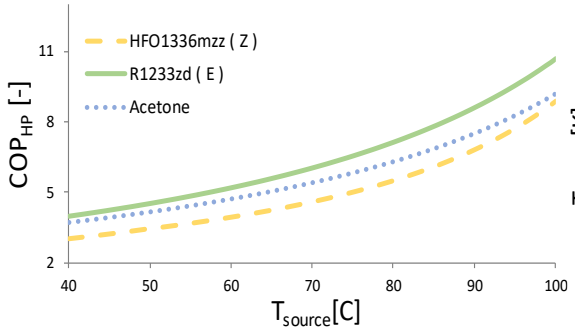

Figure 37. HP coefficient of performance, Case 1.

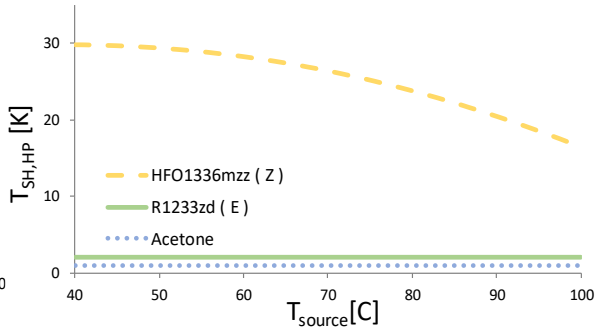

Figure 38. HP's Evaporator superheat, Case 1.

d) Organic Rankine cycle performance

The thermal efficiency and the VER of the ORC can be seen in Fig. 39. Both parameters remain constant when increasing the source temperature, for a given fixed melting and sink temperatures. HFO1336mzz(Z) has a low thermal efficiency in the ORC cycle. This has its explanation in that for a dry fluid, there is a high degree of superheat at the outlet of the expander. This can be seen clearly in Fig. 33. Acetone has the best thermal efficiency of the working fluids (17.4 %) which is about 3 unit percent higher than HFO1336mzz(Z). From Fig.33 it can also be seen that acetone has very low SH at the inlet of the condenser which has a preferable effect on the thermal efficiency. In contrast to the VHC, the VER has to be as low as possible. Therefore, Acetone is the most undesired fluid in terms of VER with a VER of 14.3.

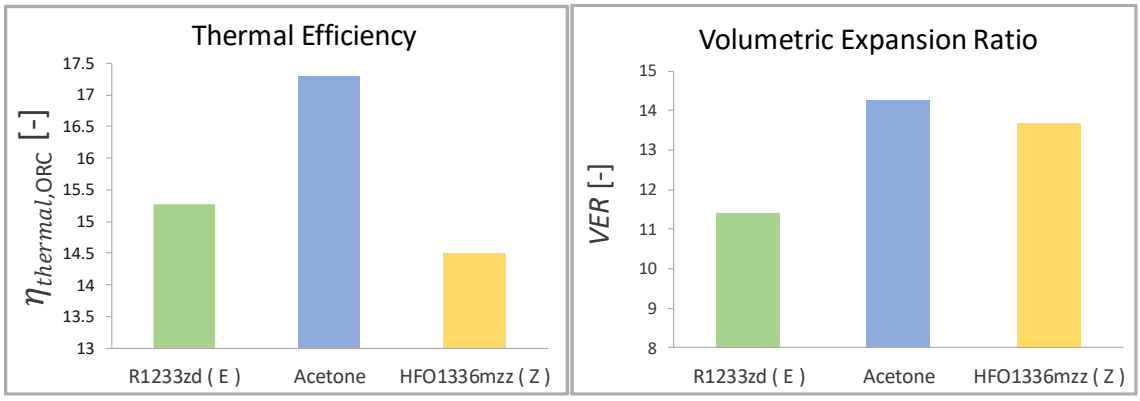

Figure 39. Thermal efficiency and volumetric expansion ratio for ORC, Case 1.

3.1.2 Case 2 (T_{melt}=149°C)

The selected fluids from Case 1 have critical temperature that is within the required range for case 2 and therefore they are kept for Case 2.

a) Cycle simulation on T-s diagram

Fig. 40 shows the T-s diagram of the system for the three selected working fluids. T_{source} was set to 70 °C and T_{melt} to 149 °C. For this case, the melting temperature is approaching the critical temperature of both R1233zd(E) and HFO1336mzz(Z) but it is still possible to use the refrigerant for Case 2. Apart from the 16 K increase of the melting temperature, the T-s diagrams are very similar to the previous case.

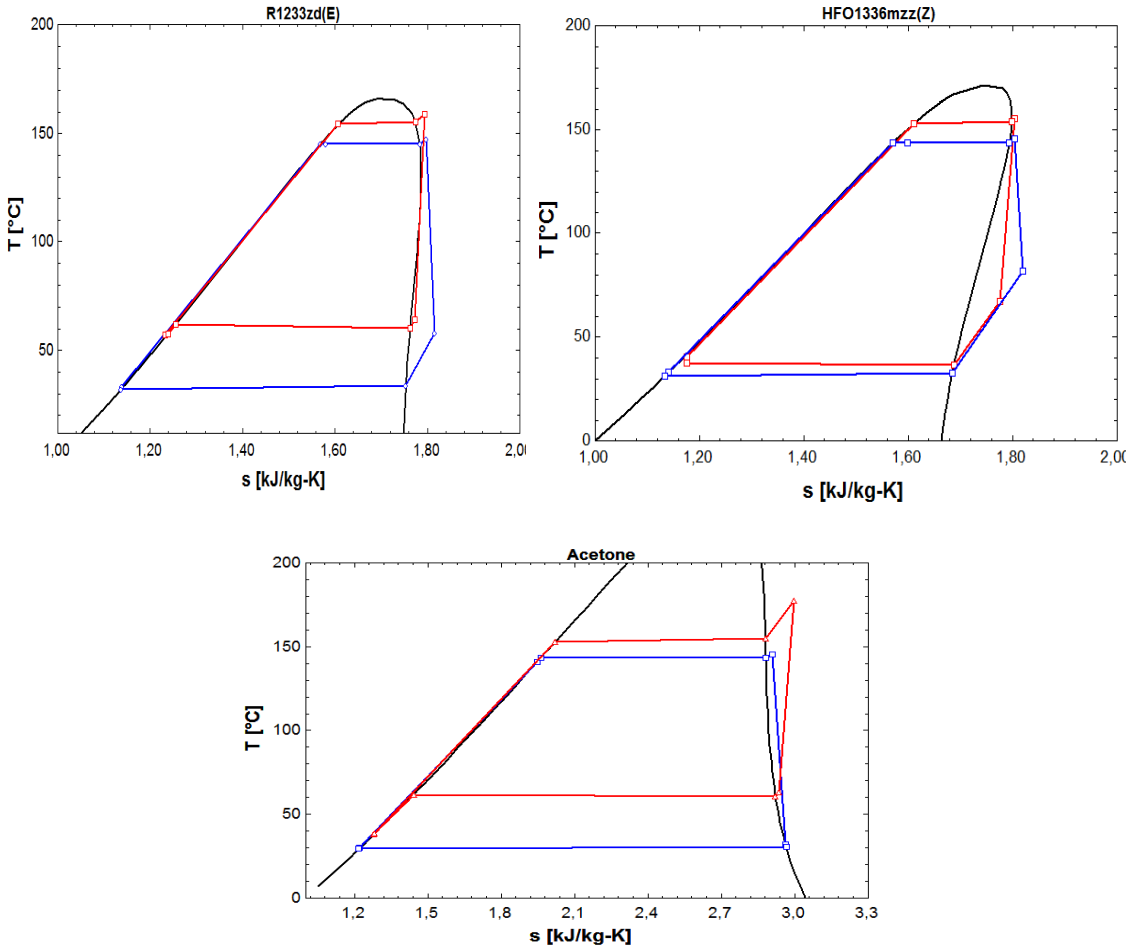

Figure 40. Cycle representation on T-s diagram for the working fluids used in Case 1, where T_{source}=70 °C.

b) Overall system performance

Fig. 41 shows the roundtrip efficiency for the Case 2. In the current case, the curvature of the graphs for roundtrip efficiency is similar to Case 1. For low source temperatures, the roundtrip is very similar to Case 1. However, for high source temperatures the roundtrip efficiency is lower for all fluids. When T_{source}=100 °C, R1233zd(E) has a roundtrip efficiency which is 11% lower in comparison to Case 1. HFO1336mmz(Z) has lower performance than the other fluid in the whole temperature range. The roundtrip efficiency of R1233zd(E) and Acetone follows each other closely.

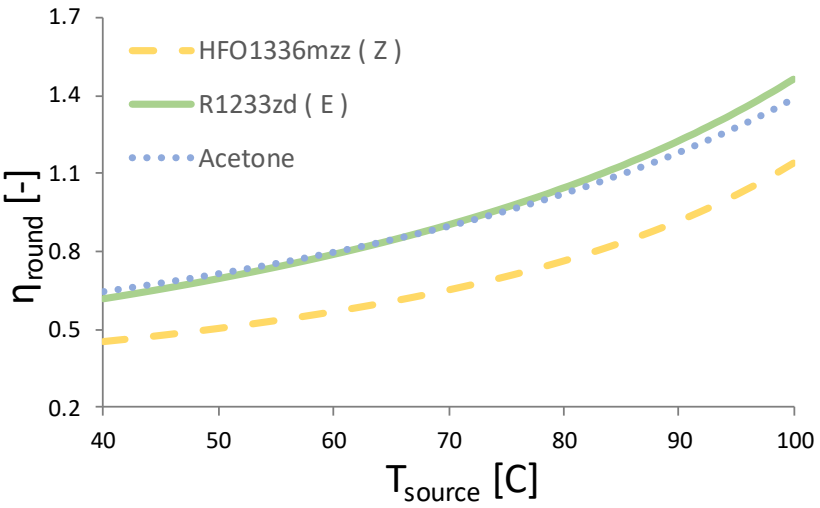

Figure 41. Roundtrip efficiency for CHEST system for Case 2.

C) Heat pump cycle performance

Fig. 42 shows the COP_{HP} as a function of the source temperature for Case 2. As expected, the COP_{HP} will be lower for the current case, compared to Case 1, due to the increase of condensation temperature. However, for low source temperatures the difference is very small. R1233zd(E) performs best of all fluids and reaches a COP_{HP} of 9.3 when T_{source}=100 °C

Fig. 43 shows the final discharge temperature for Case 2. The discharge temperature of the compressor is higher than for Case 1 and reaches 193 °C when T_{source}=40 °C. The final discharge temperature is higher for the other two fluids as well, compared to Case 1. Apart from that, the trend of the curves is similar.

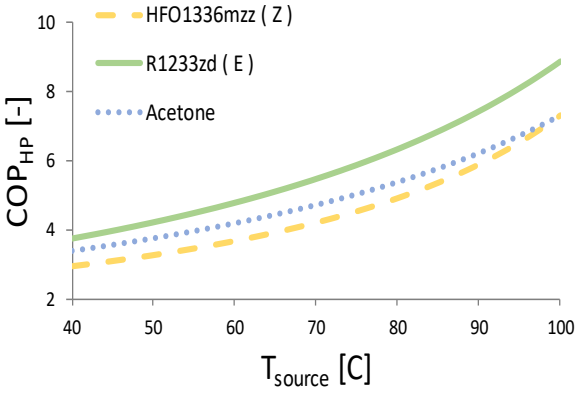

Figure 42. HP's coefficient of performance, Case 2.

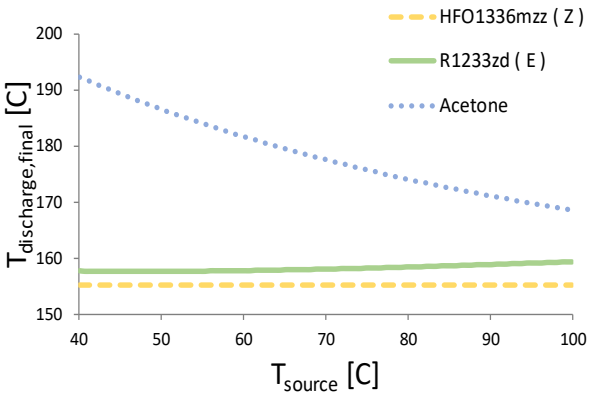

Figure 43. HP's final discharge temperature, Case 2.

Fig. 44 shows the volumetric heating capacity and is very similar to Case 1 for all fluids. The VHC for Acetone reaches a value of 800 kJ/m^3 when T_{source}=40 °C. Apart from that, the values and trends of the fluids are similar to Case 1.

Fig. 45 shows that the superheat required for HFO1336mzz(Z) in Case 2 is higher than for Case 1. When T_{source}=40 °C, 33 K superheat is needed in order to avoid wet expansion. As the source temperature increases, the necessary superheat decreases and reaches 20 K when T_{source}=40 °C.

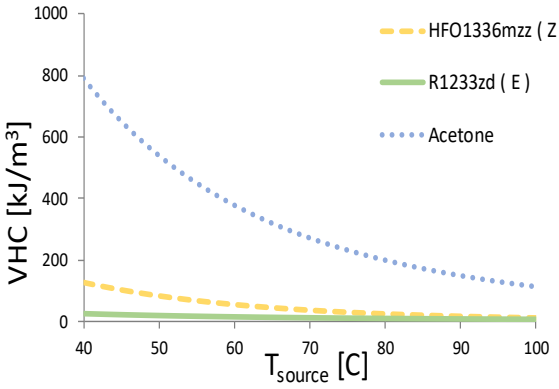

Figure 44. HP's volumetric heating capacity, Case 2.

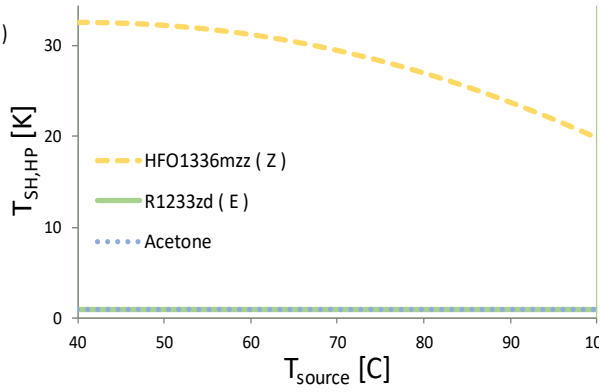

Figure 45. HP's Evaporator superheat, Case 2.

d) Organic Rankine cycle performance

The results for the ORC can be seen in Fig. 46. As expected for an ORC cycle, the thermal efficiency will be higher for Case 2. The melting temperature is higher and the discharging cycle reaches higher efficiency the larger the temperature difference between the melting temperature and the sink temperature. The VER is larger than for Case 2 than for Case 1. This is because the specific volume at the inlet of the expander is lower at high temperature.

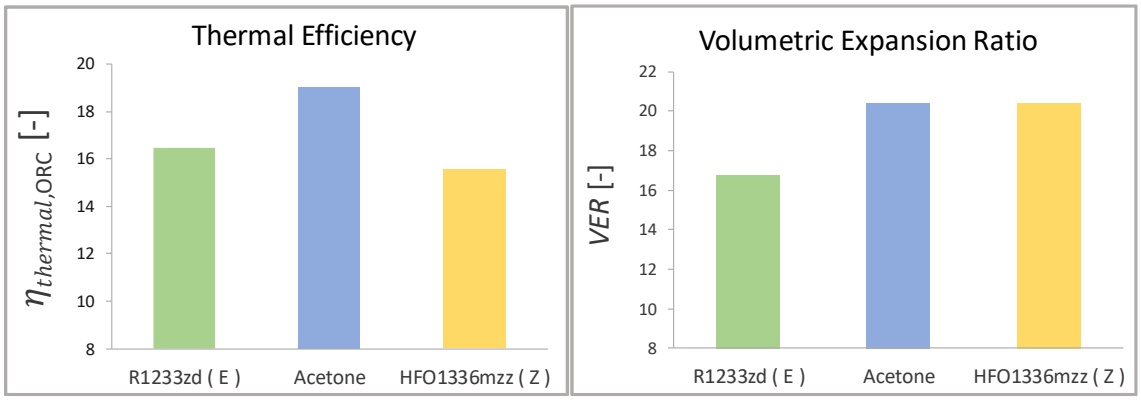

Figure 46. Thermal efficiency and volumetric expansion ratio for ORC, Case 2.

3.1.3 Case 3 (T_{melt}=183 °C)

In the current case, the dry and the isentropic fluid are changed to cyclopentane and R141b, respectively, due to their higher critical temperature. For this case, Acetone is compressed in two stages in order to see the effect on the performance indicators.

a) Cycle simulation on T-s diagram

Fig. 47 shows the system cycles on T-s diagram for the three selected working fluids. The source temperature is set to 70 °C. As for Case 1, a high degree of superheat is necessary in order to avoid wet compression for the dry fluid, cyclopentane. For R141b, which has an isentropic behavior, a small degree of superheating is necessary in order to avoid compression in the wet region. The cycle behavior of acetone does not change much from Case 1.

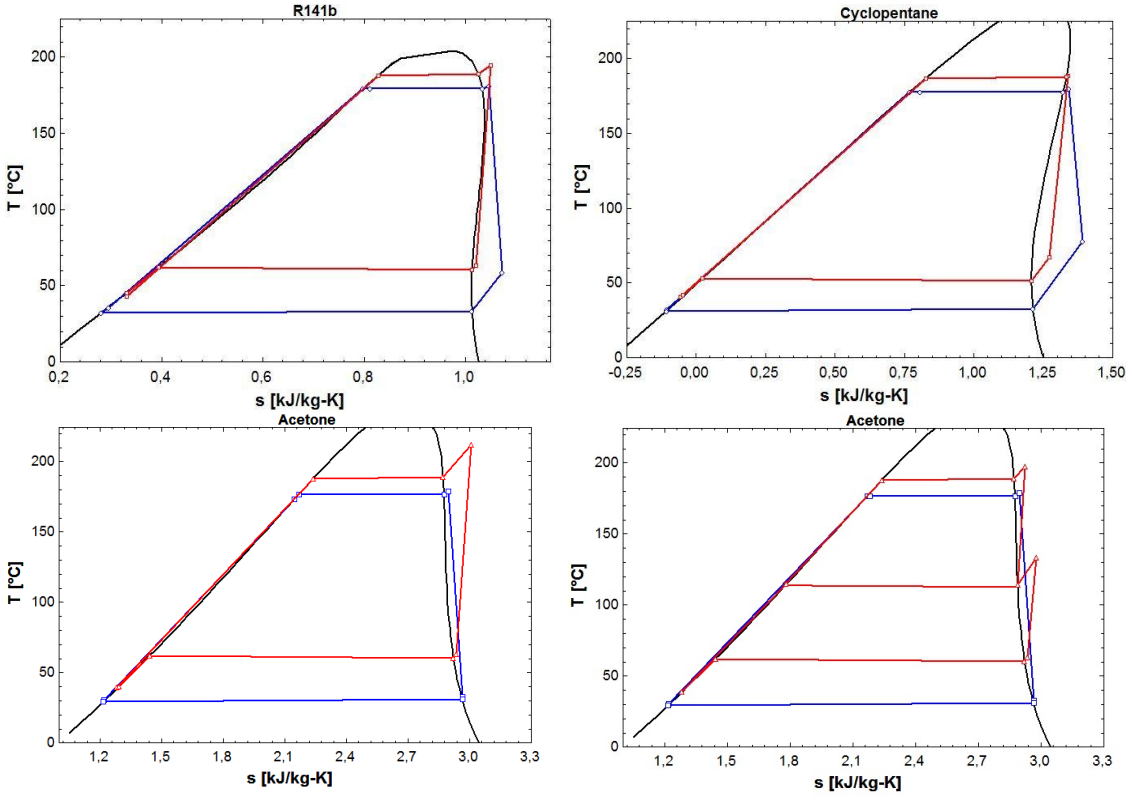

Figure 47. Cycle representation on T-s diagram for the working fluids used in Case 3, where Tsource=70 ºC .

b) Overall system performance

Fig. 48 shows the results for the roundtrip efficiency. The general trend is, as for Cases 1 and 2, the roundtrip efficiency is increased when the source temperature increases. The different working fluids follows the same trend as spotted before where Acetone and R141b follow each other very closely. From Fig. 47 it can be seen that Cyclopentane demonstrate a wet behavior in the low temperature region, hence a low degree of superheat is needed to avoid expansion in the two-phase region and the roundtrip efficiency increases. When the source temperature is increased, cyclopentane demonstrates more dry properties and therefore the roundtrip efficiency has a slower increase than for the other working fluids.

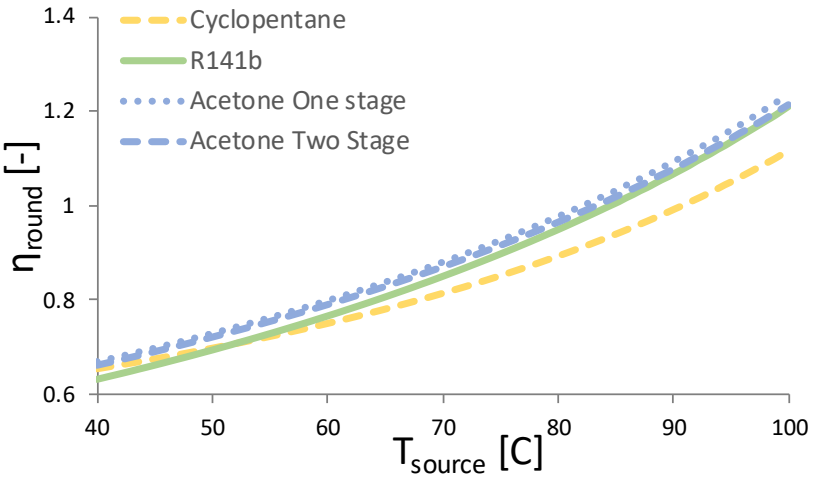

Figure 48. Roundtrip efficiency for CHEST system for Case 3.

c) Heat pump cycle performance

From Fig. 49 it can be seen that Acetone has very good VHC at low source temperatures and good VHC at high temperatures for both one and two stage compression. Cyclopentane demonstrates good VHC in the whole range and reaches 180 kJ/m^3 when T_{source}=100 °C, this is only slightly below Acetone at 190 kJ/m^3 for the same source temperature. R141b has the poorest performance of all the tested working fluids.

Fig. 50 shows that One-stage Acetone system has the highest final discharge temperature in the whole temperature range, from 227 °C to 205 °C. The final discharge temperature for Cyclopentane is very close to the condensation temperature. The difference between two-stages Acetone system and the isentropic fluid (R141b) is not substantial and in the high source temperature range (after 90 °C), Acetone has a slightly higher discharge temperature. The discharge temperature of cyclopentane is controlled the safety condition explained in section XX and therefore the discharge temperature is constant for the whole range.

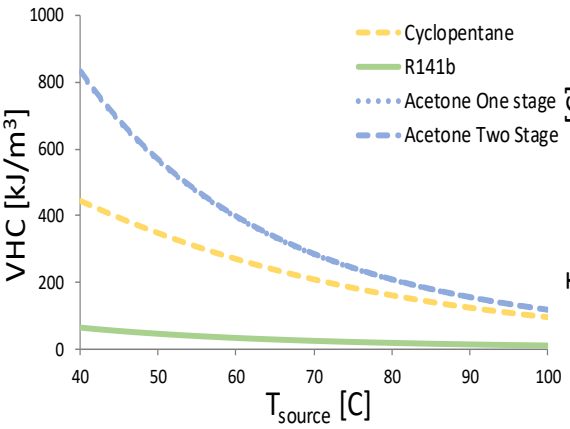

Figure 49. HP's volumetric cooling capacity, Case 3.

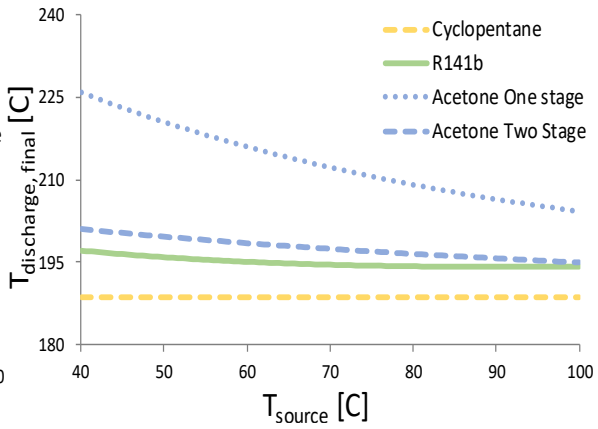

Figure 50. HP's final discharge temperature, Case 3.

In Fig. 51, the COP_{HP} of the HP can be seen for Case 3, the COP of the heat pump is lower than for cases one and two. As for Case 1 the isentropic fluid, R141b performs best for all temperature ranges. Both one and two-stage Acetone performs slightly better than Cyclopentane in the high source temperatures. Fig. 52 Shows that the superheat required for Cyclopentane is lower than for the first two Cases. Moreover, the superheat required for Cyclopentane is increasing as the source temperature increases, in contrast to HFO1336mzz(Z).

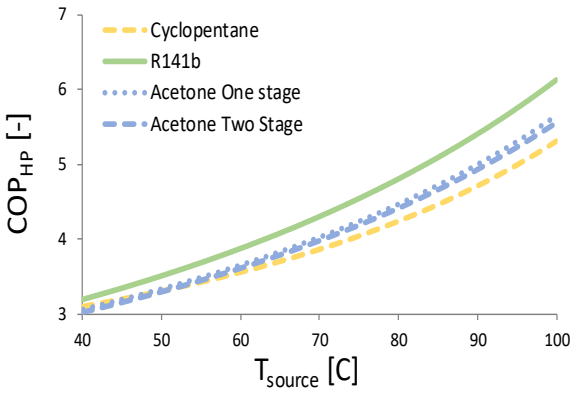

Figure 51. HP's coefficient of performance, Case 3.

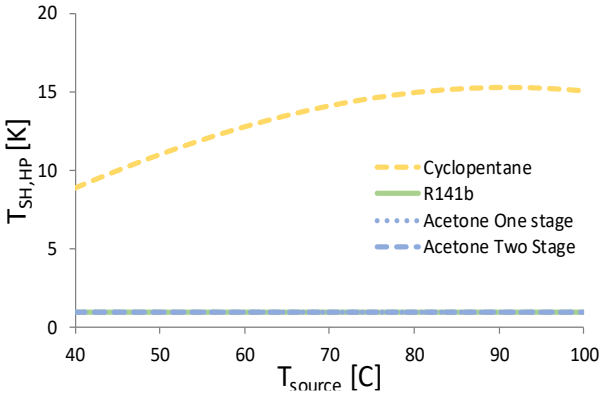

Figure 52. HP's Evaporator superheat, Case 2.

d) Organic Rankine cycle performance

The ORC has the same thermal efficiency and VER for the whole temperature range and is represented in Fig. 53. The results for the different fluids for Case 3 shows similar behavior as Case 1. Acetone has the highest thermal efficiency at 21.7 %, cylopentane has a thermal efficiency of 21.1 % and R141 has the lowest thermal efficiency at 19.7 %. Acetone has the highest VER at 42 followed by cyclopentane at 31 and R141b at 29.

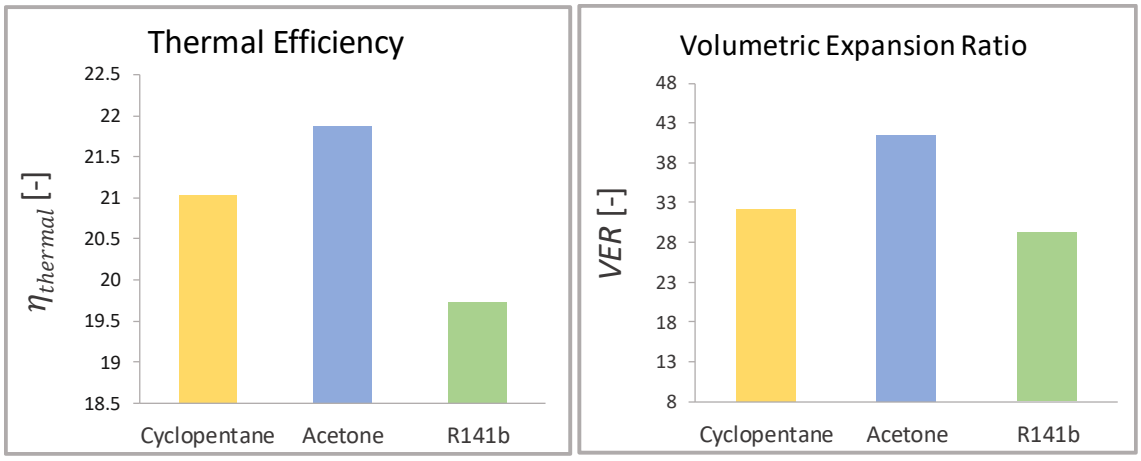

Figure 53. Thermal efficiency and volumetric expansion ratio for ORC, Case 3.

3.2 Effect of Regeneration and Recuperation Processes

This section shows the results of the roundtrip efficiency when recuperation and regeneration processes are included in the ORC. To see how recuperation and vapor bleed affect the results, Case 2 with refrigerant R1233zd(E) was chosen and the source temperature was set to 70 °C. The reasons for that is that, as shown in the previous section, the roundtrip efficiency is good for the whole temperature range and it has a low discharge temperature. Moreover, it has low GWP and is non-toxic. Therefore, it is most likely to be used in the real system.

3.2.1 ORC with regeneration

In this section, regeneration in the ORC is activated while recuperation is kept deactivated. The thermal efficiencies and the temperature difference in the SHS in are evaluated as a function of the regeneration pressure ratio. Fig. 54 shows the effect of regeneration on the system performance.

When the bleeding pressure is very close to the condensation pressure (i.e pressure ratio ≈ 0), the roundtrip efficiency is the same as in the simple ORC case. When the pressure ratio increases, the preheating of the working fluid will increase which will lead to an increase in the inlet temperature to the SHS on the ORC-side. The water temperature difference between inlet and outlet of the SHS will decrease in order to meet the safety criteria. Fig. XX also shows that the thermal efficiency of the ORC has a maximum value when the pressure ratio equals 0.25. This is because that on one side, the loss of mass flow in the expander will reduce the work output in the expander and thereby the thermal efficiency. One the other side, it has to be weighted with the increase in preheating which has a favorable effect on the thermal efficiency. The COP of the heat pump is reduced for the same reasons as for the case with recuperation - lower subcooling means lower heat stored which subsequently results to lower COP. Since the compression work from the heat pump is constant, the roundtrip efficiency is reduced because the work output from the expansion is reduced. The work output is reduced due to the loss in mass flow in the second stage expansion.

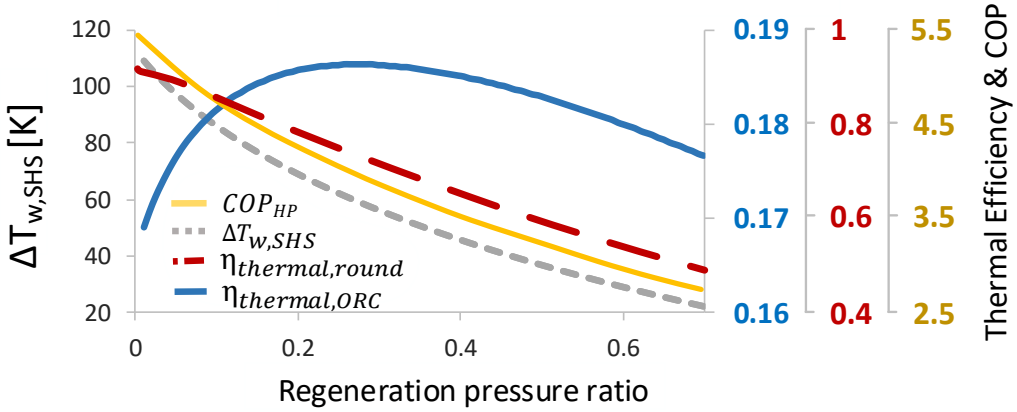

Figure 54. Effects of regeneration process on the CHEST system performance.

3.2.2 ORC with Recuperation

In this section, regeneration in the ORC is deactivated while recuperation is activated. Fig. 55 shows the effect of recuperation process on the roundtrip efficiency, ORC thermal efficiency, heat pump COP, and the water temperature difference in the SHS. As the recuperator effectiveness increases, the outlet temperature of the recuperator increases, which also means that the refrigerant temperature at the inlet of of the SHS will increase. Therefore, the water temperature difference in the SHS ($\Delta T_{w,SHS}$) should be decreased in order to fulfil the safety criteria explained in section 2.8. The thermal efficiency of the ORC will increase when adding a recuperator, due to more heat recovery. However, Fig.55 also shows that the COP_{HP} will decrease when increasing the effectiveness of the Recuperator. The explanation for this is that the subcooling in the heat pump cycle will decrease when more heat is recovered in the ORC. The total roundtrip efficiency will be kept constant no matter the recuperator effectiveness because the efficiency gains in the ORC will be reduced by the efficiency loss in the HP.

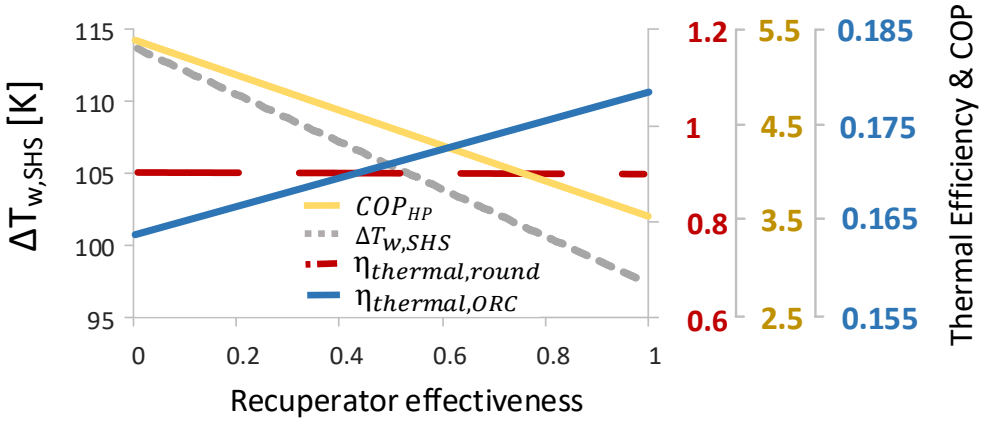

Figure 55. Effect of an increasing recuperator efficiency and the effect on roundtrip efficiency.

3.3 Parametric Study on Pinch Point Temperature and Pressure Drop in Heat Exchangers

In the following section, Case 2 has been selected and R1233zdE has been selected based on the same reasons explained in the section above.

3.3.1 Pinch Point Analysis

In Fig. 56, the influence of a higher pinch point temperature on the roundtrip efficiency for three different heat exchangers (source, LHS, and sink) in the system can be seen. The pinch point temperature has been increased for each heat exchanger while kept constant for other two heat exchangers. For the LHS, the pinch point difference is increased simultaneously on the HP- and ORC-side. Since 3 K is set as the minimum pinch point difference in the general model, the roundtrip efficiency starts at 0.9 for all heat exchangers. This same efficiency can be seen in Fig. 41 for R1233zdE at 70 ^{o} C. As expected, the roundtrip efficiency decreases for all heat exchangers when the pinch point temperature is increased. However, the decrease is larger for the source and sink temperature heat exchangers. Increasing the pinch point results to more irreversibilities that, in turn, result to an exergy destruction according to the second law of thermodynamics.

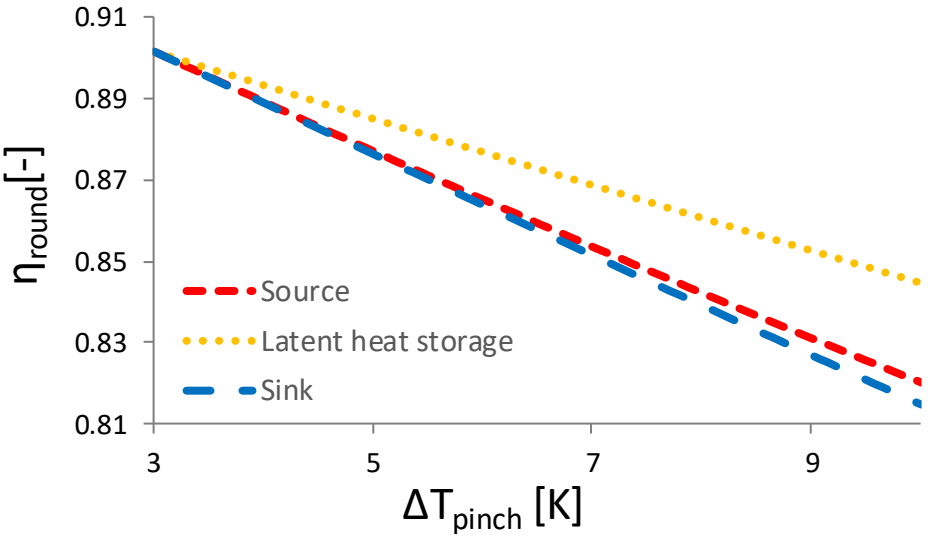

Figure 56. Roundtrip efficiency Vs. pinch points in heat exchangers.

3.3.2 Pressure Drop Analysis

In Fig. 57, the roundtrip efficiency can be seen as a function of pressure drop in the system heat exchangers. Since a 5% pressure drop is assumed for all heat exchangers in the general model, the roundtrip efficiency is 0.90 at this pressure drop value. This is because the pressure is higher in the LHS compared to the source and sink heat exchangers. The results show that the source heat exchanger is most sensitive for pressure drop. With no pressure drop, the roundtrip efficiency is at 0.93 for the source. Accordingly, the pressure drop does not affect the LHS and sink heat exchanger as much as the source. The sink heat exchanger is barely affected by a 5% pressure drop.

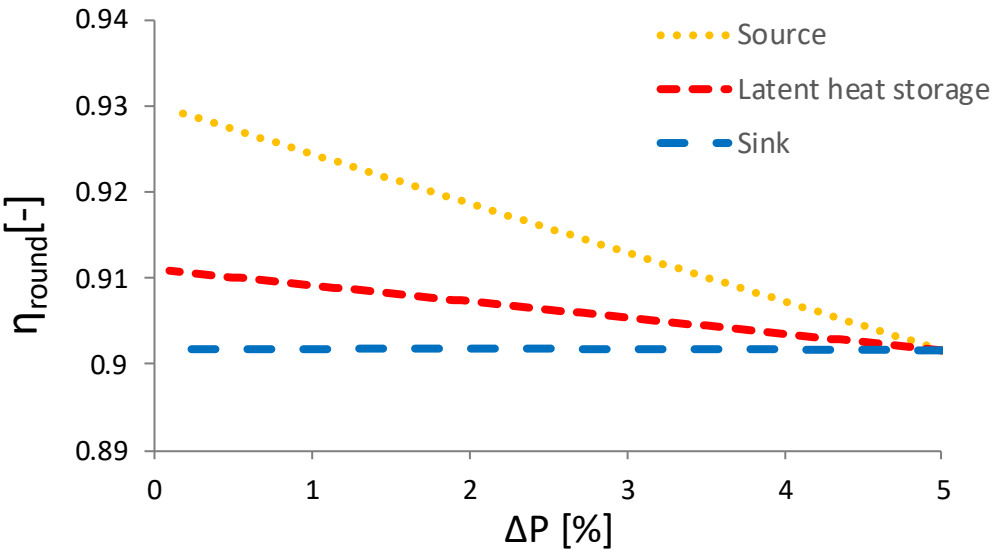

Figure 57. Roundtrip efficiency Vs. pressure drop in heat exchangers.

4. CONCLUSIONS AND FUTURE WORK

4.1 CONCLUSIONS

This work has been focused on building a thermodynamic model of a heat energy storage system and optimizing it by comparing different working fluids and system layouts. Although the project is in an early phase, some conclusion can be drawn regarding the general system configuration and possible operating fluids.

For the first scenario (Case 1), when the melting temperature was set to 133 ^{o}C, R1233zd(E) is considered the best fluid due to its high total roundtrip efficiency, low discharge temperature and its low GWP value. A roundtrip efficiency of 1 is reached when the source temperature is 74 ^{o}C. This means that, the efficiencies of the CHESTER system has the possibility be competitive to the efficiencies of other energy storage technologies. However, more detailed calculations are needed in order to draw more certain conclusions regarding this issue. The dry fluid, HFO1336mzz(Z), requires 30 K of superheat when T_{source}=40 ^{o}C in order to reach saturated conditions in the outlet of the compressor. The superheat remains very high for the whole source temperature range. A high degree of superheat degrades the evaporation temperature and heat pump COP, and therefore, the fluid discarded. Acetone has a good roundtrip efficiency, very good VHC but the discharge temperature is very high for the single stage compression.

The trends of the second scenario (Case 2) is very similar to the first one. Therefore, R1233zd(E) is still considered to be the most suitable fluid in this case. The roundtrip efficiency of the system is lower in the second case than in the first one and R1233zd(E) reaches 1 when T_{source}=80 ^{o}C. Since the only parameter that is changed is the melting temperature, it can be concluded that a higher melting temperature is not necessary in order to reach higher roundtrip efficiency. However, the roundtrip efficiency is a product of the compression work in the HP and the expander work output in the ORC. This means that for very small temperature lifts in the HP, the roundtrip will be very good. Therefore, it is necessary to note that for cases with low temperature lift, the roundtrip efficiency might not be the best indicator of efficiency.

In the third scenario (Case 3) the melting temperature is raised considerably making it necessary to change two of the fluids. However, independent of the new fluids, the isentropic fluid performs best in this case as well. R141b reaches a roundtrip efficiency of 1 when T_{source}=86 ^{o}C. Moreover, it is shown that the discharge temperature and pressure ratio could be decreased by adopting two-stage compression. Due to the increasing cycle complexity of a two-stage compression, many parameters must be favorable if such a system should be implemented.

As a general conclusion, the results of three cases studied indicate that isentropic fluids are preferable for the CHEST system. This conclusion can be drawn in regard to that the dry fluids which require high superheat, which subsequently reduce roundtrip efficiency; and the wet fluids that result to high discharge temperature which can affect the performance of lubrication oil and damage the compressor. The benefits of implementing a two-stage compression is not considered to be larger than the disadvantages. The only problem with the isentropic fluids tested are the low values of VHC which indicates large compressor sizes. However, these results need to be investigated further to draw any certain conclusions.

In the second part of the results, the effect of recuperation and regeneration process is analyzed. The most important conclusion is that it will not be beneficial for the roundtrip efficiency to

include regeneration or recuperation process in the CHEST system. This conclusions is valid as long as most of the subcooled liquid in the HP is used for the SHS and later, to preheat the ORC.

The third part of the results includes the effect of pressure drop and pinch point temperature on the roundtrip efficiency. As expected, a higher pinch point temperature have a negative effect on the roundtrip efficiency. The sink and the source heat exchangers has an 11% reduction of roundtrip efficiency and are most effected by larger pinch point difference. Therefore, the design and selection of heat exchangers, especially source and sink heat exchangers are crucial and affect significantly on the overall system performance.

The source if affected most by a pressure drop. Therefore, it can be noticed that especial effort should be put in the design of the heat exchanger in the source heat exchangers in order to avoid high pressure drops could have a high impact on the roundtrip efficiency.

4.2 FUTURE WORK

This work has focused on the preliminary thermodynamic model of the CHEST system. Much work remains until the model is ready to be used as a base for a real prototype. A more detailed of the HP is required in order to size the components. Future work should also include transient operation. Time has not been included in the calculations so far and it is necessary in order to evaluate the performance and operation of the thermal storage unit. From an operational point of view, the best would be to store the heat as long as possible in order to wait for high demand of electricity or low renewable electricity production.

The heat exchangers also need to be dimensioned and a more detailed mathematical model should be developed for them, using for example LMTD or ε-NTU method. The compressor and the expander also need to be sized to obtain performance correlations that can be used to calculate more realistic values for efficiencies.

REFERENCES

[1] "Technology Options," 2018. [Online]. Available: http://www.esru.strath.ac.uk/EandE/Web_sites/14-15/Industrial_autonomy/2_1_technology_options.html. [Accessed: 06-Mar-2018].

[2] M. Aneke and M. Wang, "Energy storage technologies and real life applications – A state of the art review," *Appl. Energy*, vol. 179, pp. 350–377, 2016.

[3] "Compressed Heat Energy Storage for Energy from Renewable sources. Project ID: 764042," 2018. [Online]. Available: https://cordis.europa.eu/project/rcn/214061_en.html. [Accessed: 05-Jul-2018].

[4] S. Feja, C. Hanzelmann, and S. Zuber, "PT and viscosity measurements of High-Temperature Ammonia Heat Pump Lubricants," *Int. J. Refrig.*, vol. 88, pp. 221–228, 2018.

[5] E. Granryd, I. Ekroth, P. Lundqvist, A. Melinder, B. Palm, and P. Rohlin, *Refrigeration Engineering*, 4th ed. Stockholm: Department of Energy Technology, Division of Applied Thermodynamics and Refrigeration, Royal Institute of Technology, KTH, 2003.

[6] *Lesson 12 Multi-Stage Vapour Compression Refrigeration Systems*, Version 1. IIT Kharagpur.

[7] C. Arpagaus, F. Bless, M. Uhlmann, J. Schiffmann, and S. S. Bertsch, "High temperature heat pumps: Market overview, state of the art, research status, refrigerants, and application potentials," *Energy*, vol. 152, 2018.

[8] Group Viking Development, "Viking Heat Engines," 2018. [Online]. Available: http://www.vikingheatengines.com/heatbooster. [Accessed: 07-May-2018].

[9] M. Chamoun, R. Rulliere, P. Haberschill, and J. L. Peureux, "Experimental and numerical investigations of a new high temperature heat pump for industrial heat recovery using water as refrigerant," *Int. J. Refrig.*, vol. 44, pp. 177–188, 2014.

[10] B. Vanslambrouck, "Energetical, Technical and Economical considerations by choosing between a Steam and an Organic Rankine Cycle for Small Scale Power Generation," 2011.

[11] H. Ohman, "Organic Rankine Cycles, Low Temperature Power Cycles," 2016.

[12] S. Lecompte, H. Huisseune, M. Van Den Broek, B. Vanslambrouck, and M. De Paepe, "Review of organic Rankine cycle (ORC) architectures for waste heat recovery," *Renew. Sustain. Energy Rev.*, vol. 47, pp. 448–461, 2015.

[13] Z. Li *et al.*, "Comparison study of Trilateral Rankine Cycle, Organic Flash Cycle and basic Organic Rankine Cycle for low grade heat recovery," *Energy Procedia*, vol. 142, pp. 1441–1447, 2017.

[14] B. Dong, G. Xu, T. Li, Y. Quan, and J. Wen, "Thermodynamic and economic analysis of zeotropic mixtures as working fluids in low temperature organic Rankine cycles," *Appl. Therm. Eng.*, vol. 132, pp. 545–553, 2018.

[15] K. Braimakis and S. Karellas, "Energetic optimization of regenerative Organic Rankine Cycle (ORC) configurations," *Energy Convers. Manag.*, vol. 159, no. September 2017, pp.

353–370, 2018.

[16] H. Xi, M. J. Li, C. Xu, and Y. L. He, “Parametric optimization of regenerative organic Rankine cycle (ORC) for low grade waste heat recovery using genetic algorithm,” *Energy*, vol. 58, pp. 473–482, 2013.

[17] J. Nouman, “Comparative studies and analyses of working fluids for Organic Rankine Cycles - ORC,” 2012.

[18] H. Jockenhöfer, W. D. Steinmann, and D. Bauer, “Detailed numerical investigation of a pumped thermal energy storage with low temperature heat integration,” *Energy*, vol. 145, pp. 665–676, 2018.

[19] K. H. Kim, “Effects of Superheating on Thermodynamic performance of regenerative organic Rankine cycles,” *Eng. Technol.*, vol. 59, no. 6, pp. 1515–1519, 2011.

[20] A. Groniewsky, G. Györke, and A. R. Imre, “Description of wet-to-dry transition in model ORC working fluids,” *Appl. Therm. Eng.*, vol. 125, pp. 963–971, 2017.

[21] G. Alva, Y. Lin, and G. Fang, “An overview of thermal energy storage systems,” *Energy*, vol. 144, pp. 341–378, 2018.

[22] W. D. Steinmann, “The CHEST (Compressed Heat Energy STorage) concept for facility scale thermo mechanical energy storage,” *Energy*, vol. 69, pp. 543–552, 2014.

[23] P. J. Mago, L. M. Chamra, K. Srinivasan, and C. Somayaji, “An examination of regenerative organic Rankine cycles using dry fluids,” *Appl. Therm. Eng.*, vol. 28, no. 8–9, pp. 998–1007, 2008.

[24] R. Rayegan and Y. X. Tao, “A procedure to select working fluids for Solar Organic Rankine Cycles (ORCs),” *Renew. Energy*, vol. 36, no. 2, pp. 659–670, 2011.

[25] A. Dinker, M. Agarwal, and G. D. Agarwal, “Heat storage materials, geometry and applications: A review,” *J. Energy Inst.*, vol. 90, no. 1, pp. 1–11, 2017.

[26] J. Pereira da Cunha and P. Eames, “Thermal energy storage for low and medium temperature applications using phase change materials - A review,” *Appl. Energy*, vol. 177, pp. 227–238, 2016.

[27] B. J. Woodland, A. Krishna, E. A. Groll, J. E. Braun, W. T. Horton, and S. V. Garimella, “Thermodynamic comparison of organic Rankine cycles employing liquid-flooded expansion or a solution circuit,” *Appl. Therm. Eng.*, vol. 61, no. 2, pp. 859–865, 2013.

[28] ipcc, “IPCC Fourth Assessment Report: Climate Change 2007,” 2007. [Online]. Available: https://www.ipcc.ch/publications_and_data/ar4/wg1/en/ch2s2-10-3-2.html. [Accessed: 06-Jun-2018].

[29] J. Xu and C. Yu, “Critical temperature criterion for selection of working fluids for subcritical pressure Organic Rankine cycles,” *Energy*, vol. 74, no. C, pp. 719–733, 2014.

[30] D. Wang, X. Ling, H. Peng, L. Liu, and L. L. Tao, “Efficiency and optimal performance evaluation of organic Rankine cycle for low grade waste heat power generation,” *Energy*, vol. 50, no. 1, pp. 343–352, 2013.

[31] Linde Group, “R123.” [Online]. Available: http://www.linde-gas.com/en/products_and_supply/refrigerants/hcfc_refrigerants/r123/index.html.

[32] L. Daikin Industries, “HCFC-141b,” 2019. [Online]. Available: https://www.daikin.com/chm/products/pdfDown.php?url=pdf/tds/tds_hcfc141b_e.pdf. [Accessed: 05-Jul-2018].

[33] M. Welzl, F. Heberle, and D. Brüggemann, “Simultaneous experimental investigation of nucleate boiling heat transfer and power output in ORC using R245fa and R1233zd(E),” *Energy Procedia*, vol. 129, pp. 435–442, 2017.

[34] “A year in low GWP refrigerants development,” 2016. [Online]. Available: https://www.kth.se/en/itm/inst/energiteknik/forskning/ett/projekt/koldmedier-med-lag-gwp/low-gwp-news/utvecklingen-pa-koldmediefronten-under-aret-som-gatt-1.636006.

[35] R. Nagata, C. Kondou, and S. Koyama, “Comparative assessment of condensation and pool boiling heat transfer on horizontal plain single tubes for R1234ze(E), R1234ze(Z), and R1233zd(E),” *Int. J. Refrig.*, vol. 63, pp. 157–170, 2016.

[36] “R1336mzz-Z - new generation nonflammable low GWP refrigerant,” 2014. [Online]. Available: https://www.kth.se/en/itm/inst/energiteknik/forskning/ett/projekt/koldmedier-med-lag-gwp/low-gwp-news/r1336mzz-z-ett-nytt-hogtemperaturkoldmedium-med-bra-egenskaper-1.501202. [Accessed: 06-Jun-2018].

[37] “Refrigerants - Environmental Properties.” [Online]. Available: https://www.engineeringtoolbox.com/Refrigerants-Environment-Properties-d_1220.html. [Accessed: 05-Jul-2018].

[38] “Reducing Greenhouse Gas Emissions at GE’s Refrigerator Manufacturing Facilities,” 2011. [Online]. Available: http://pressroom.geappliances.com/news/reducing-greenhouse-gas-emissions-190718. [Accessed: 05-Jul-2018].

[39] E. Macchi and M. Astolfi, *Organic Rankine Cycle (ORC) Power Systems Technologies and Applications*. Elsevier, 2017.

APPENDIX

A. SYSTEM PARAMETERS

All the parameters that are used in the system are shown here with corresponding value

A1. Parameters for the Charging Cycle

Table 4. Parameters for the Charging cycle.

Parameter	Substitute name	Value	Unit
Isentropic compressor efficiency	η_{comp}	0.8	[-]
Isentropic pump efficiency	η_{pump}	0.8	[-]
Recuperator efficiency	ε_{rec}	0.9	[-]
Inlet source temperature	$T_{source,in}$	variable	[C]
Outlet of source temperature	$T_{source,out}$	variable	[C]
Source Temperature difference in	ΔT_{source}	5	[K]
Temperature difference source outlet and saturated vapour in condenser	$\Delta T_{sink,pinch}$	5	[K]
Superheat in evaporator	$\Delta_{T,evap,sh,HP}$	5	[K]
Difference between temperature of PCM and outlet of evaporator	$\Delta_{T,evap,pinch}$	5	[K]
Pressure drop in heat exchangers	ΔP_{hex}	8	[%]
Intermediate pressure level	P_{bleed}	variable	[kPa]

A2. Parameters for the Discharging Cycle

Table 5. Parameters for the Discharging cycle

Parameter	Substitute name	Value	Unit
Isentropic expander efficiency	$\eta_{exp,efficiency}$	0.8	[-]
Isentropic pump efficiency	$\eta_{pump,efficiency}$	0.8	[-]
Recuperator efficiency	ε_{rec}	0.9	[-]
Inlet of sink	$T_{sink,in}$	variable	[C]
Outlet of sink	$T_{sink,out}$	25	[C]
Temperature difference in sink	ΔT_{sink}	5	[K]
Temperature difference sink outlet and saturated vapour in condenser	$\Delta T_{sink,pinch}$	5	[K]
Superheat in evaporator	$\Delta T_{ORC,evap,sh}$	5	[K]
Difference between temperature of PCM and outlet of evaporator	$\Delta T_{evap,pinch}$	5	[K]
Pressure drop in heat exchangers	ΔP_{hex}	50	[kPa]
Intermediate pressure level	P_{bleed}	variable	[kPa]

B. EES CODE AND DIAGRAM WINDOW.

The diagram window and the EES code used for R1233zd(E) and source temperature of 70 °C. Are shown in this section. The program can easily be altered to work for all the scenarios explained in the report.

B1. Diagram window

First part of the Diagram Window.

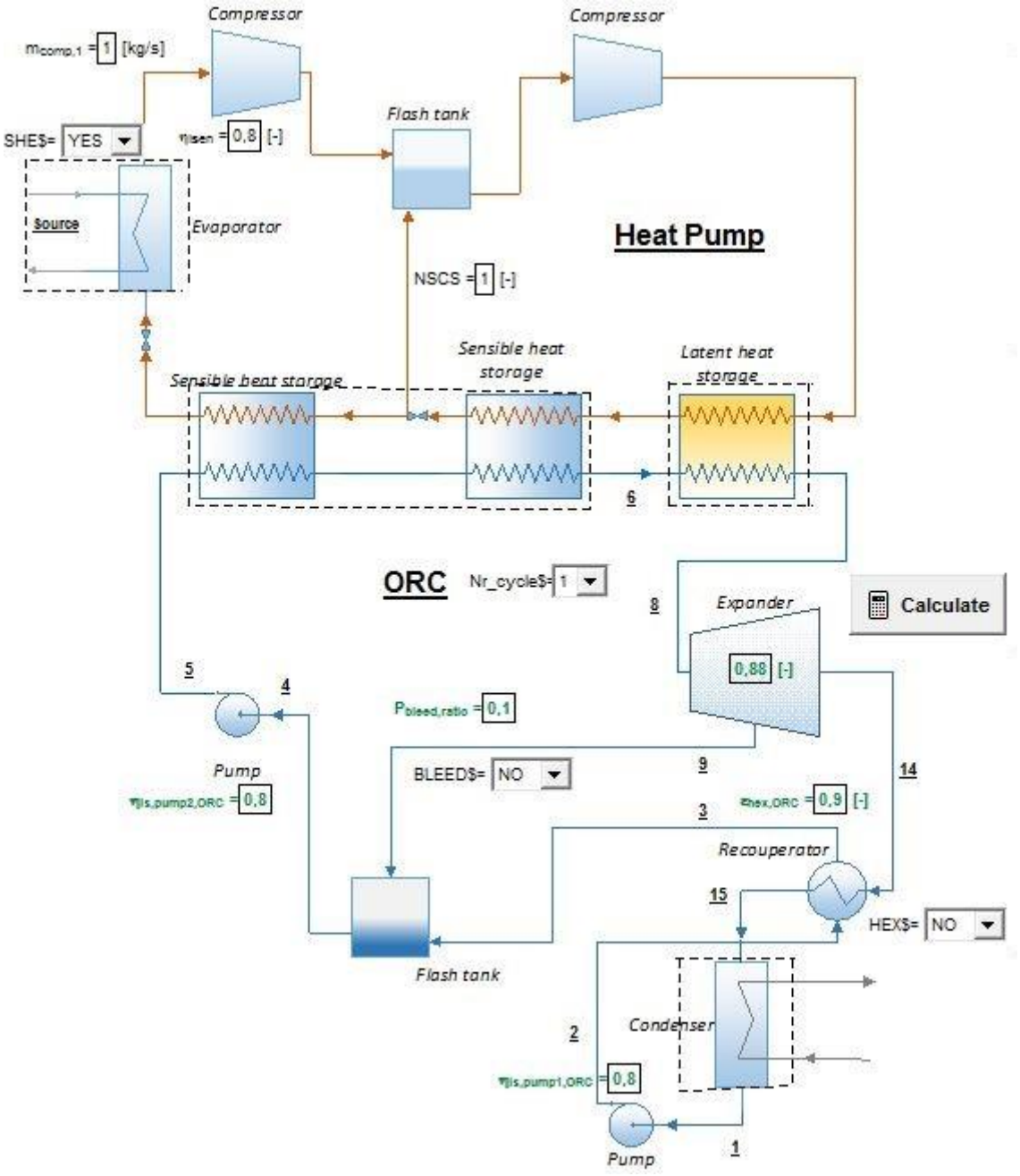

Figure 58. First part of diagram window.

Second part of the diagram window

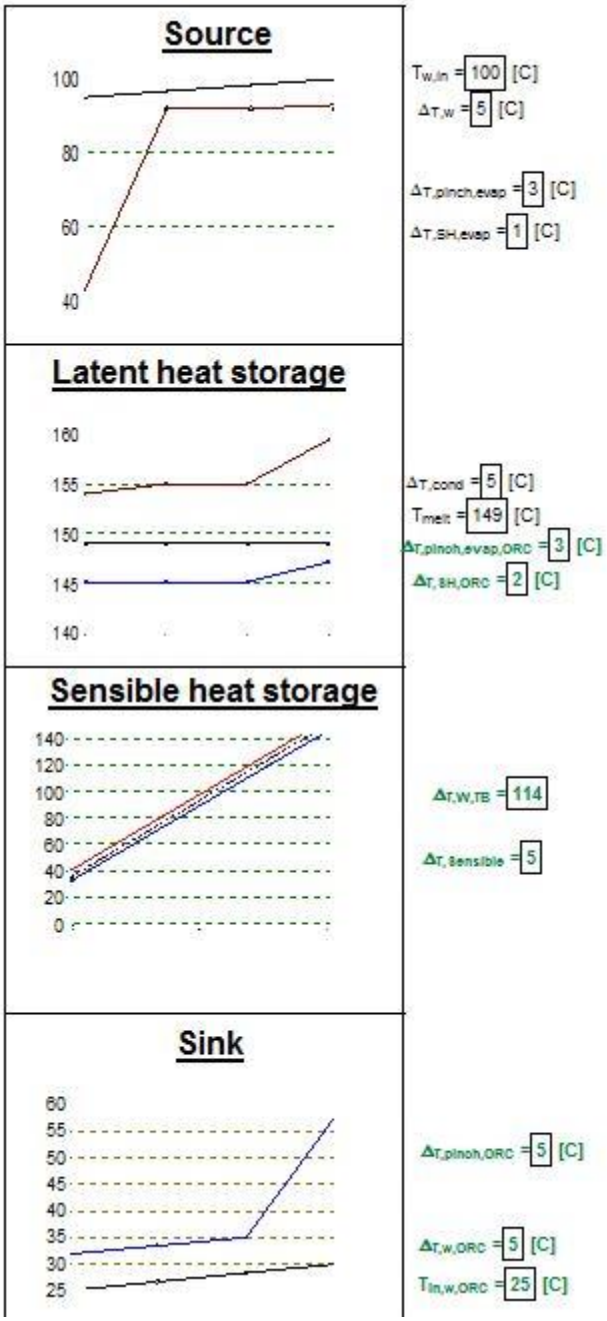

Figure 59. Second part of diagram window

B2. EES code

```
{ DELTA_T_pinch_evap}
{ m_comp_1}
{ eta_isen}
{NCSC}
{ T_w_in}
{ DELTA_T_w}
{ DELTA_T_pinch_evap}
{ DELTA_T_SH_evap}
{ DELTA_T_cond}
{ T_melt}
{ eta_isen_ORC}
{ epsilon_HEX_ORC}
{ eta_isen_Pump1_ORC}
{eta_isen_Pump1_ORC}
{ T_w_in}
{ DELTA_T_bw}
{ DELTA_T_w_pinch_ORC}
{SH=Yes}
{ m_comp_1}

Ref$='R1233zd(E)'
    "Refrigerant"
DELTA_P_evap=P_evap*0,05
    "Pressure drop in kPa"
DELTA_P_cond=50
    "Pressure drop"
DELTA_P_evap_ORC=50
    "Pressure drop"
DELTA_P_cond_ORC=P_cond_ORC*0,05
    "Pressure drop in kPa"
T_w_out=T_w_in - DELTA_T_w
    "Temperature of source outlet"
T_cond=T_melt+DELTA_T_cond+1
    "Condensation temperature, +1 to compensate for pressure drop"
P_evap=pressure(Ref$;T=T_evap;x=0)
    "Evaporating pressure"
T_evap=T_w_out-
DELTA_T_pinch_evap
    "Evaporation Temperature"
P_cond=p_sat(Ref$;T=T_cond)
    "Condensation pressure"
NSC=NSCS
    "Number of compression stages"
NP=(4*NSC)+2
    "Total number of cycle points"
Duplicate j=1;NSC
Eta_is[j]=Eta_isen
    "Compressor efficiency"
End
    "Safety Variables for Criteria"
Safety_T_bot=T_bot-T_ORC[5]
Safety_T_top=T[NSC*2+2]-T_top
Safety_Sink=T_ORC[1]-T_in_w_ORC
Safety_Melt=T[NSC*2+2]-T_melt
Safety_Source=T_w_in-T[1]
Safety_two_phase=h[NSC*2]-h[NSC*2+1]
Safety_SH_ORC_OUTLET=T_melt-T_ORC[8]
```

```
x[0]=0
    "Imaginary distance in a Heat exchanger"
x[1]=1
x[2]=2
x[3]=3
T_draw_w[0]=T_w_out
    "Temperature profile: Source"
T_draw_w[1]=(T_draw_w[0]+T_draw_w[2])/2
T_draw_w[2]=(T_draw_w[1]+T_draw_w[3])/2
T_draw_w[3]=T_w_in
T_draw_evap[0]=T[NSC*4+2]
    "Temperature profile: Evaporator"
T_draw_evap[1]=T_evap
T_draw_evap[2]=T_evap
T_draw_evap[3]=T[1]
T_draw_evap_sat[0]=T_evap
    "Temperature profile: Evaporation Temperaure"
T_draw_evap_sat[1]=(T_draw_evap_sat[0]+T_draw_evap_sat[2])/2
T_draw_evap_sat[2]=(T_draw_evap_sat[1]+T_draw_evap_sat[3])/2
T_draw_evap_sat[3]=T_evap
T_draw_melt[0]=T_melt
    "Temperature profile: Melting Temperaure"
T_draw_melt[1]=T_melt
T_draw_melt[2]=T_melt
T_draw_melt[3]=T_melt
T_draw_cond[3]=T[NSC*2]
    "Temperature profile: Condensation HP"
T_draw_cond[2]=T_cond
T_draw_cond[1]=T_cond
T_draw_cond[0]=T[NSC*2+2]
T_draw_evap_ORC[0]=T_ORC[6]
    "Temperature profile: Evaporation ORC"
T_draw_evap_ORC[1]=T_ORC[7]
T_draw_evap_ORC[2]=T_ORC[7]
T_draw_evap_ORC[3]=T_ORC[8]
    "Draw just to make figure work, bugg"
T_control[1]=T_ORC[6]-5
T_control[2]=T_ORC[6]-5
T_control[3]=T_ORC[6]-5
T_control[4]=T_ORC[6]-5
T_draw_w_ORC[0]=T_in_w_ORC
    "Temperature profile: Sink"
T_draw_w_ORC[1]=(T_draw_w_ORC[2]+T_draw_w_ORC[0])/2
T_draw_w_ORC[2]=(T_draw_w_ORC[1]+T_draw_w_ORC[3])/2
T_draw_w_ORC[3]=T_out_w_ORC
T_draw_cond_ORC[0]=T_ORC[1]
    "Temperature profile: Condensation ORC"
T_draw_cond_ORC[1]=(T_draw_cond_ORC[0]+T_draw_cond_ORC[2])/2
T_draw_cond_ORC[2]=T_cond_ORC
T_draw_cond_ORC[3]=T_ORC[15]
T_draw_rec_HT_ORC[0]=T_ORC[15]
    "Temperature profile: Recuperator"
T_draw_rec_HT_ORC[1]=T_ORC[14]
T_draw_rec_LT_ORC[0]=T_ORC[2]
    "Temperature profile: Recuperator"
T_draw_rec_LT_ORC[1]=T_ORC[3]
ORC_drawT[1]=T_ORC[1]
    "Temperature profile:T-s Diagram. To draw the cycle so that fluid reaches saturated
conditions and not cross the saturated liquid line"
ORC_drawT[2]=T_ORC[2]
```

```
ORC_drawT[3]=T_ORC[3]
ORC_drawT[4]=T_ORC[4]
ORC_drawT[5]=T_ORC[5]
ORC_drawT[6]=if(entropy(ref_ORC$;P=P_ORC[6];x=0);s_ORC[6];temperature(ref_ORC$;P=
P_ORC[6];x=0);T_ORC[6];T_ORC[6])
ORC_drawT[7]=if(entropy(ref_ORC$;P=P_ORC[6];x=0);s_ORC[6];T_ORC[6];T_ORC[6];temp
erature(ref_ORC$;P=P_ORC[6];x=0))
ORC_drawT[8]=T_ORC[7]
ORC_drawT[9]=T_ORC[8]
ORC_drawT[10]=T_ORC[9]
ORC_drawT[11]=T_ORC[10]
ORC_drawT[12]=T_ORC[11]
ORC_drawT[13]=T_ORC[12]
ORC_drawT[14]=T_ORC[13]
ORC_drawT[15]=T_ORC[14]
ORC_drawT[16]=T_ORC[15]
ORC_drawT[17]=T_ORC[16]
ORC_drawT[18]=T_ORC[17]
ORC_drawT[19]=T_ORC[18]
ORC_draws[1]=s_ORC[1]
ORC_draws[2]=s_ORC[2]
ORC_draws[3]=s_ORC[3]
ORC_draws[4]=s_ORC[4]
ORC_draws[5]=s_ORC[5]
ORC_draws[6]=if(entropy(ref_ORC$;P=P_ORC[6];x=0);s_ORC[6];entropy(ref_ORC$;P=P_O
RC[6];x=0);s_ORC[6];s_ORC[6])
ORC_draws[7]=if(entropy(ref_ORC$;P=P_ORC[6];x=0);s_ORC[6];s_ORC[6];s_ORC[6];entrop
y(ref_ORC$;P=P_ORC[6];x=0))
ORC_draws[8]=s_ORC[7]
ORC_draws[9]=s_ORC[8]
ORC_draws[10]=s_ORC[9]
ORC_draws[11]=s_ORC[10]
ORC_draws[12]=s_ORC[11]
ORC_draws[13]=s_ORC[12]
ORC_draws[14]=s_ORC[13]
ORC_draws[15]=s_ORC[14]
ORC_draws[16]=s_ORC[15]
ORC_draws[17]=s_ORC[16]
ORC_draws[18]=s_ORC[17]
ORC_draws[19]=s_ORC[18]
    "The SHS is drawn"
Sensible_draw_ORC[0]=T_ORC[5]
Sensible_draw_ORC[1]=T_ORC[6]
Sensible_draw_[0]=T_bot
Sensible_draw_[1]=T_top
Sensible_draw_HP[0]=T[NSC*4+1]
Sensible_draw_HP[1]=T[NSC*2+2]

 Duplicate j=1;NSC
    "Calculating pressures and intermedate pressures based on the defined temperatures"
      P[2*j-1]=(P_evap*(P_cond/P_evap)^((j-1)/NSC))-DELTA_P_evap
End
 Duplicate j=1;NSC
      P[2*j]=P_evap*(P_cond/P_evap)^(j/NSC)
    "Assuming similar pressure ratios"
End
 Duplicate j=1;NSC
       P[NP+1-2*j]= P[NP-2*j]-50
    "Inlet Pressures from Expansion Valves, pressure drop"
```

```
End
 Duplicate j=1;NSC
       P[NP+2-2*j]= P[2*j-1]+DELTA_P_evap
    "Outlet Pressures from Expansion Valves, pressure drop"
End
Duplicate j=2;NSC
m_inject[j-1]=m_comp[j-1]*((h[2*j-2]-h[2*j-2+1])/(h[2*j-2+1]-h[NP+2-2*j]))
    "Calculations of mass flow"
m_comp[j]=m_comp[j-1]+m_inject[j-1]
End
    "Saturated conditions in evaporator"
h[0]=enthalpy(Ref$;P=P[0];x=1)
T[0]=temperature(Ref$;P=P[0];x=1)
v[0]=volume(Ref$;P=P[0];x=1)
s[0]=entropy(Ref$;P=P[0];x=1)
$IF
SHE$='YES'
    "If superheat in included"
P[1]=P[0]
T[1]=T_evap+DELTA_T_SH_evap
h[1]=enthalpy(Ref$;P=P[1];T=T[1])
v[1]=volume(Ref$;P=P[1];h=h[1])
s[1]=entropy(Ref$;P=P[1];h=h[1])
$ELSE
h[1]=h[0]
T[1]=T[0]
v[1]=v[0]
s[1]=s[0]
$ENDIF
Duplicate j=1;NSC
    "Inlet to compressor, Saturated vapour"
h[2*j-1+2]=enthalpy(Ref$;P=P[2*j-1+2];x=1)
T[2*j-1+2]=temperature(Ref$;P=P[2*j-1+2];x=1)
v[2*j-1+2]= volume(Ref$;P=P[2*j-1+2];x=1)
s[2*j-1+2]=entropy(Ref$;P=P[2*j-1+2];x=1)
End
Duplicate
j=1;NSC
    "Outlet of compressor"
s_is[2*j]=s[2*j-1]
    "Isentropic properties"
h_is[2*j]=enthalpy(Ref$;P=P[2*j];s=s_is[2*j])
h[2*j]=h[2*j-1]+((h_is[2*j]-h[2*j-1])/(Eta_is[j]))
    "Actual properties with isentropic efficiency"
T[2*j]=temperature(Ref$;P=P[2*j];h=h[2*j])
v[2*j]=volume(Ref$;P=P[2*j];h=h[2*j])
s[2*j]=entropy(Ref$;P=P[2*j];h=h[2*j])
End
P[2*NSC+1]=P[2*NSC]+(P[2*NSC+2]-P[2*NSC])*(h[2*NSC+1]-h[2*NSC])/(h[2*NSC+2]-
h[2*NSC])
    "Inlet Properties to the LHS, after superheat"
h[2*NSC+1]=enthalpy(Ref$;P=P[2*NSC+1];x=1)
T[2*NSC+1]=temperature(Ref$;P=P[2*NSC+1];x=1)
v[2*NSC+1]=volume(Ref$;P=P[2*NSC+1];x=1)
s[2*NSC+1]=entropy(Ref$;P=P[2*NSC+1];x=1)
P[2*NSC+2]=P[2*NSC]DELTA_P_cond
    "Outlet Properties to the LHS"
h[2*NSC+2]=enthalpy(Ref$;P=P[2*NSC+2];x=0)
T[2*NSC+2]=temperature(Ref$;P=P[2*NSC+2];x=0)
v[2*NSC+2]=volume(Ref$;P=P[2*NSC+2];x=0)
```

```
s[2*NSC+2]=entropy(Ref$;P=P[2*NSC+2];x=0)
$IF
Nr_cycle$='1'
    "IF conditions depending on number of cycles"
    "Subcooling storage and inlet to evaporator"
h[5]=enthalpy(Ref$;T=T[5];P=P[5])
v[5] =volume(Ref$;P=P[5];h=h[5])
s[5] =entropy(Ref$;P=P[5];h=h[5])
h[6]=h[5]
T[6]=temperature(Ref$;P=P[6];h=h[6])
v[6]=volume(Ref$;P=P[6];h=h[6])
s[6]=entropy(Ref$;P=P[6];h=h[6])
$ENDIF
$IF Nr_cycle$='2'
h[7]=h[8]
T[7]=temperature(Ref$;h=h[7];P=P[7])
    "Subcooling storage and inlet to evaporator"
v[7] =volume(Ref$;P=P[7];h=h[7])
s[7] =entropy(Ref$;P=P[7];h=h[7])
h[8]=enthalpy(Ref$;P=P[8];x=0)
T[8]=temperature(Ref$;P=P[8];h=h[8])
v[8]=volume(Ref$;P=P[8];h=h[8])
s[8]=entropy(Ref$;P=P[8];h=h[8])
h[9]=enthalpy(Ref$;P=P[9];T=T[9])
v[9]=volume(Ref$;P=P[9];h=h[9])
s[9]=entropy(Ref$;P=P[9];h=h[9])
h[10]=h[9]
T[10]=temperature(Ref$;P=P[10];h=h[10])
v[10]=volume(Ref$;P=P[10];h=h[10])
s[10]=entropy(Ref$;P=P[10];h=h[10])
$ENDIF
$IF
Nr_cycle$='3'
    "IF conditions depending on number of cycles"
h[9]=h[10]
T[9]=temperature(Ref$;P=P[9];h=h[9])
    "Subcooling storage and inlet to evaporator"
v[9] =volume(Ref$;P=P[9];h=h[9])
s[9] =entropy(Ref$;P=P[9];h=h[9])
h[10]=enthalpy(Ref$;P=P[10];x=0)
T[10]=temperature(Ref$;P=P[10];h=h[10])
v[10]=volume(Ref$;P=P[10];h=h[10])
s[10]=entropy(Ref$;P=P[10];h=h[10])
h[11]=h[12]
T[11]=temperature(Ref$;P=P[11];h=h[11])
    "Subcooling storage and inlet to evaporator"
v[11] =volume(Ref$;P=P[11];h=h[11])
s[11] =entropy(Ref$;P=P[11];h=h[11])
h[12]=enthalpy(Ref$;P=P[12];x=0)
T[12]=temperature(Ref$;P=P[12];h=h[12])
v[12]=volume(Ref$;P=P[12];h=h[12])
s[12]=entropy(Ref$;P=P[12];h=h[12])
h[13]=enthalpy(Ref$;P=P[13];T=T[13])
v[13]=volume(Ref$;P=P[13];h=h[13])
s[13]=entropy(Ref$;P=P[13];h=h[13])
h[14]=h[13]
T[14]=temperature(Ref$;P=P[14];h=h[14])
v[14]=volume(Ref$;P=P[14];h=h[14])
s[14]=entropy(Ref$;P=P[14];h=h[14])
$ENDIF
```

```
P[NP+1]=P[NP]+(P[NP+2]-P[NP])*(h[NP+1]-h[NP])/(h[NP+2]-h[NP])
    "For DRAWING y1=y0+(y2-y0)*(x1-x0)/(x2-x0) - Linear interpolation"
h[NP+1]=if(h[4*NSC+2];enthalpy(Ref$;P=P[NP+1];x=0);enthalpy(Ref$;P=P[NP+1];x=0);h[3*N
SC+2];h[3*NSC+2])
s[NP+1]=entropy(Ref$;P=P[NP+1];h=h[NP+1])
T[NP+1]=temperature(Ref$;P=P[NP+1];h=h[NP+1])
P[NP+2]=P[0]
    "Virtual Point to Close the Cycle"
h[NP+2]=h[0]
T[NP+2]=T[0]
v[NP+2]=v[0]
s[NP+2]=s[0]
Duplicate j=1;NSC
SC[j]=T[NP-2*j]-T[NP+1-2*j]
    "Subcooling"
End
SC_tot=sum(SC[j]; j=1;NSC)
    "Total summation of subcooling"
Duplicate j=1;NSC
W_comp[j]=m_comp[j]*(h[2*j]-h[2*j-1])
    "Work copressor"
End
W_comp_tot=sum(W_comp[j]; j=1;NSC)
    "Total compressor work"
Q_evap=m_comp[1]*(h[1]-h[NP])
    "Cooling Capacity"
Q_SHS=m_comp[NSC]*(h[2*NSC]-h[2*NSC+1])
    "Capacity of superheating heat storage at Pcond"
Q_LHS=m_comp[NSC]*(h[2*NSC+1]-h[2*NSC+2])
    "Capacity of LHS at Pcond"
Duplicate j=1;NSC
Q_SCS[j]=m_comp[NSC-j+1]*(h[2*NSC+j*2]-h[2*NSC+j*2+1])
    "Summary of each subcooling storage unit"
End
Q_SCS_tot=sum(Q_SCS[j]; j=1;NSC)
    "Total capacity for subcooling storage modules"
Q_HST_tot=Q_SHS+Q_LHS+Q_SCS_tot
    "Total heat storage capacity"
COP_heat=Q_HST_tot/W_comp_tot
    "Heating COP"
Q_SCHS_ORC=Q_SCS_tot
    "Total Subcooling heat from ORC is equal to total subcooling heat from HP"
Q_Upper_Heat_ORC=Q_LHS+Q_SHS
    "Total upper heat (Latent storage unit) of ORC is equal to total Latent + The small amount of
superheat from HP"
Q_Upper_Heat_ORC=m_dot_ref_ORC*(h_ORC[8]-
h_ORC[6])                                        "Mass flow of ORC is determined"
Q_SCHS_ORC=m_dot_ref_ORC*(h_ORC[6]-
h_ORC[5])
    "Enthalpy of ORC at Inlet of latent heat / Outlet of Sensible heat is calculated"
    // For heat exchange in SHS
T_ORC[6]=T_top-
DELTA_T_Sensible
    "Equations for defining the SHS"
T[NSC*4+1]=T_bot+DELTA_T_Sensible
DELTA_T_W_TB=T_top-T_bot
ref_ORC$=Ref$
    "ORC refrigerant"
```

```
P_atm_ORC=1013,25
T_out_w_ORC=T_in_w_ORC+DELTA_T_w_ORC
    "Outlet temperature of the water"
T_evap_ORC=T_melt-DELTA_T_pinch_evap_ORC-DELTA_T_SH_ORC
    "Evaporation temperature of ORC"
P_evap_ORC=p_sat(ref_ORC$;T=T_evap_ORC)
    "Evaporation pressure of ORC"
T_cond_ORC=T_out_w_ORC+DELTA_T_pinch_ORC
    "Evaporation pressure of ORC"
P_cond_ORC=p_sat(ref_ORC$;T=T_cond_ORC)
    "Condensation tempaerature of ORC"
P_bleed_ORC=(P_evap_ORC-
P_cond_ORC)*P_bleed_ratio+P_cond_ORC
    "Define the bleeding pressure"
    "Before pump 1"
P_ORC[1]=P_cond_ORC-2*DELTA_P_cond_ORC
h_ORC[1]=enthalpy(ref_ORC$;P=P_ORC[1];x=0)
s_ORC[1]=entropy(ref_ORC$;P=P_ORC[1];x=0)
T_ORC[1]=t_sat(ref_ORC$;P=P_ORC[1])
$IF
Bleed$='YES'
    "Conditions if bleed is activated"
P_ORC[2]=P_bleed_ORC-DELTA_P
$ELSE
P_ORC[2]=P_evap_ORC+2*DELTA_P_evap_ORC
$ENDIF
h_2_is_ORC=enthalpy(ref_ORC$;P=P_ORC[2];s=s_ORC[1])
    "Isentropic value"
h_ORC[2]=(h_2_is_ORC-h_ORC[1])/eta_is_pump1_ORC+h_ORC[1]
s_ORC[2]=entropy(ref_ORC$;P=P_ORC[2];h=h_ORC[2])
T_ORC[2]=temperature(ref_ORC$;P=P_ORC[2];s=s_ORC[2])
P_ORC[3]=P_ORC[2]
    "Recuperation value"
s_ORC[3]=entropy(ref_ORC$;P= P_ORC[3];h=h_ORC[3])
T_ORC[3]=temperature(ref_ORC$;s=s_ORC[3];P=P_ORC[3])
h_3_prim_ORC=enthalpy(ref_ORC$;T=T_ORC[14];P=P_ORC[3])
    "Enthalpy of SC liquid at the temperature after expansion, used to calculate maximum
efficiency of the recouperator"
$IF
Bleed$='YES'
    "If bleed is activated"
X_mass_ORC=(h_ORC[4]-h_ORC[3])/(h_ORC[9]-
h_ORC[3])                                   "Energy balance over the regenerator
where X_mass=m_flow_bleed/m_flow_tot"
P_ORC[4]=P_bleed_ORC -DELTA_P
h_ORC[4]=enthalpy(ref_ORC$;P= P_ORC[4];x=0)
s_ORC[4]=entropy(ref_ORC$;P= P_ORC[4];x=0)
T_ORC[4]=temperature(ref_ORC$;P=P_ORC[4];x=0)
P_ORC[5]=P_evap_ORC
    "Inlet to LHS"
h_5_is_ORC=enthalpy(ref_ORC$;P=P_ORC[5];s=s_ORC[4])
h_ORC[5]=(h_5_is_ORC-h_ORC[4])/eta_is_pump2_ORC+h_ORC[4]
s_ORC[5]=entropy(ref_ORC$;P=P_ORC[5];h=h_ORC[5])
T_ORC[5]=temperature(ref_ORC$;P=P_ORC[5];s=s_ORC[5])
$ELSE
P_ORC[4]=P_ORC[3]
s_ORC[4]=s_ORC[3]
T_ORC[4]=T_ORC[3]
h_ORC[4]=h_ORC[3]
```

```
P_ORC[5]=P_ORC[3]
s_ORC[5]=s_ORC[3]
T_ORC[5]=T_ORC[3]
h_ORC[5]=h_ORC[3]
 $ENDIF
P_ORC[6]=P_evap_ORC+DELTA_P_evap_ORC
s_ORC[6]=entropy(ref_ORC$;P= P_ORC[6];h=h_ORC[6])
T_ORC[6]=temperature(ref_ORC$;P=P_ORC[6];h=h_ORC[6])
P_ORC[7]=P_ORC[6]+(P_ORC[8]-P_ORC[6])*(h_ORC[7]-h_ORC[6])/(h_ORC[8]-h_ORC[6])
    " For drawing: y1=y0+(y2-y0)*(x1-x0)/(x2-x0) - Linear interpolation"
h_ORC[7]=enthalpy(ref_ORC$;P=P_ORC[7];x=1)
    "Saturated vapor"
s_ORC[7]=entropy(ref_ORC$;P= P_ORC[7];x=1)
T_ORC[7]=temperature(ref_ORC$;P=P_ORC[6];x=1)
    "Superheated vapor"
P_ORC[8]=P_evap_ORC
s_ORC[8]=entropy(ref_ORC$;P=P_ORC[8];h=h_ORC[8])
h_ORC[8]=enthalpy(ref_ORC$;P=P_ORC[8];T=T_ORC[8])
T_ORC[8]=T_ORC[7]+DELTA_T_SH_ORC
v_8= volume(ref_ORC$;P=P_ORC[8];T=T_ORC[8])
$IF
Bleed$='YES'
    "Conditions if bleed is included"
P_ORC[9]=P_bleed_ORC
h_9_is_ORC=enthalpy(ref_ORC$;P=P_ORC[9];s=s_ORC[8])
eta_is_expander_ORC=((h_ORC[8]-h_ORC[9])+(1-X_mass_ORC)*(h_ORC[9]-
h_ORC[14]))/((h_ORC[8]-h_9_is_ORC)+(1-X_mass_ORC)*(h_9_is_ORC-h_14_is_ORC)) "To
calculate the enthalpy at the bleed point with the efficiency of the expander"
s_ORC[9]=entropy(ref_ORC$;P=P_ORC[9];h=h_ORC[9])
T_ORC[9]=temperature(ref_ORC$;h=h_ORC[9];s=s_ORC[9])
    "Point for drawing line to regenerator"
P_ORC[10]=P_ORC[9]+(P_ORC[11]-P_ORC[9])*(s_ORC[10]-s_ORC[9])/(s_ORC[11]-
s_ORC[9])
h_ORC[10]=enthalpy(ref_ORC$;P= P_ORC[10];x=1)
s_ORC[10]=entropy(ref_ORC$;P= P_ORC[10];x=1)
T_ORC[10]=temperature(ref_ORC$;P=P_ORC[10];x=1)
    "Point for drawing line to regenerator"
P_ORC[11]=P_ORC[4]
h_ORC[11]=h_ORC[4]
s_ORC[11]=s_ORC[4]
T_ORC[11]=T_ORC[4]
    "Point for drawing line to regenerator"
P_ORC[12]=P_ORC[10]
h_ORC[12]=h_ORC[10]
s_ORC[12]=s_ORC[10]
T_ORC[12]=T_ORC[10]
    "Point for drawing line to regenerator"
P_ORC[13]=P_ORC[9]
h_ORC[13]=h_ORC[9]
s_ORC[13]=s_ORC[9]
T_ORC[13]=T_ORC[9]
    "Outlet of recouperator"
$ELSE
    "If not bleed is activated"
    "Many point are excluded if bleed is not included"
P_ORC[9]=P_ORC[8]
s_ORC[9]=s_ORC[8]
T_ORC[9]=T_ORC[8]
h_ORC[9]=h_ORC[8]
```

```
P_ORC[10]=P_ORC[8]
s_ORC[10]=s_ORC[8]
T_ORC[10]=T_ORC[8]
h_ORC[10]=h_ORC[8]
P_ORC[11]=P_ORC[8]
s_ORC[11]=s_ORC[8]
T_ORC[11]=T_ORC[8]
h_ORC[11]=h_ORC[8]
P_ORC[12]=P_ORC[8]
s_ORC[12]=s_ORC[8]
T_ORC[12]=T_ORC[8]
h_ORC[12]=h_ORC[8]
P_ORC[13]=P_ORC[8]
s_ORC[13]=s_ORC[8]
T_ORC[13]=T_ORC[8]
h_ORC[13]=h_ORC[8]
    "After Regenerator"
$ENDIF
    "After expansion & inlet to recouperator"
P_ORC[14]=P_cond_ORC
h_14_is_ORC=enthalpy(ref_ORC$;P=P_ORC[14];s=s_ORC[8])
h_ORC[14]=h_ORC[8]-(h_ORC[8]-h_14_is_ORC)*eta_is_expander_ORC
s_ORC[14]=entropy(ref_ORC$;P=P_ORC[14];h=h_ORC[14])
T_ORC[14]=temperature(ref_ORC$;h=h_ORC[14];s=s_ORC[14])
v_14= volume(ref_ORC$;P=P_ORC[14];T=T_ORC[14])
$IF
HEX$='YES'
    "Possiblility to add recouperator or not"
P_ORC[15]=P_ORC[14]-DELTA_P_cond_ORC
s_ORC[15]=entropy(ref_ORC$;P=P_ORC[15];h=h_ORC[15])
T_ORC[15]=temperature(ref_ORC$;h=h_ORC[15];s=s_ORC[15])
epsilon_hex_ORC=(h_ORC[14]-h_ORC[15])/(h_ORC[14]-h_ORC[16])
     "Largest heat transfer possible in case of low bleed pressure"
h_ORC[14]-h_ORC[15]=h_ORC[3]-h_ORC[2]
    "Mass balance Recouperator"
$ELSE
P_ORC[15]=P_ORC[14]
s_ORC[15]=s_ORC[14]
h_ORC[15]=h_ORC[14]
T_ORC[15]=T_ORC[14]
h_ORC[3]=h_ORC[2]
$ENDIF
    "Exit of recouperator"
P_ORC[16]=P_ORC[14]-DELTA_P_cond_ORC
    "y1=y0+(y2-y0)*(x1-x0)/(x2-x0) - Linear interpolation"
h_ORC[16]=enthalpy(ref_ORC$;P=P_ORC[16];x=1)
s_ORC[16]=entropy(ref_ORC$;P=P_ORC[16];x=1)
T_ORC[16]=temperature(ref_ORC$;P=P_ORC[16];x=1)
    "Point to close the cycle"
P_ORC[17]=P_ORC[18]
h_ORC[17]=h_ORC[18]
s_ORC[17]=s_ORC[18]
T_ORC[17]=T_ORC[18]
    "Point for bugg in the system"
P_ORC[1]=P_ORC[18]
h_ORC[1]=h_ORC[18]
s_ORC[1]=s_ORC[18]
T_ORC[1]=T_ORC[18]

q_in_ORC=h_ORC[8]-h_ORC[5]
```

```
$IF Bleed$='YES'
    "Taking into account if there is a loss of mass flow in turbine or not"
work_net_ORC=(h_ORC[8]-h_ORC[9])+(1-X_mass_ORC)*(h_ORC[9]-h_ORC[14])-(1-
X_mass_ORC)*(h_ORC[2]-h_ORC[1])-(h_ORC[5]-h_ORC[4])
$ELSE
work_net_ORC=(h_ORC[8]-h_ORC[14])-(h_ORC[2]-h_ORC[1])-(h_ORC[5]-h_ORC[4])
$ENDIF
eta_thermal_ORC=work_net_ORC/q_in_ORC
 eta_thermal_round=(work_net_ORC*m_dot_ref_ORC)/W_comp_tot
 T_discharge=T[NSC*2]
VHC=Q_HST_tot*v[1]
VER=v_14/v_8
 VCC=(h[1]-h[NSC*4+2])/v[1]
```